ANTHROPOMOPRPHICALLY INSPIRED DESIGN OF A TENDON-DRIVEN ROBOTIC PROSTHESIS FOR HAND IMPAIRMENTS

by

Manali Bapurao Bhadugale
B.E. May 2009, Solapur University, India

A Thesis Submitted to the Faculty of
Old Dominion University in Partial Fulfillment of the
Requirements for the Degree of

MASTER OF SCIENCE

MECHANICAL ENGINEERING

OLD DOMINION UNIVERSITY
May 2018

Approved by:

Krishnanand Kaipa (Director)

Sebastian Bawab (Member)

Julie Hao (Member)

ABSTRACT

ANTHROPOMOPRPHICALLY INSPIRED DESIGN OF A TENDON-DRIVEN
ROBOTIC PROSTHESIS FOR HAND IMPAIRMENTS

Manali Bapurao Bhadugale
Old Dominion University, 2018
Director: Dr. Krishnanand Kaipa

This thesis presents the design of a robotic prosthesis, which mimics the morphology of a human hand. The primary goal of this work is to develop a systematic methodology that allows a custom-build of the prosthesis to match the specific requirements of a person with hand impairments. Two principal research questions are addressed toward this goal: 1) How do we cater to the large variation in the distribution of overall hand-sizes in the human population? 2) How closely do we mimic the complex morphological aspects of a biological hand in order to maximize the anthropomorphism (human-like appearance) of the robotic hand, while still maintaining a customizable and manageable design? This design approach attempts to replicate the crucial morphological aspects in the artificial hand (the kinematic structure of the hand skeleton, the shape and aspect ratios of various bone-segments, and ranges of motion). The hand design is partitioned into two parts: 1) A stiff skeleton structure, comprising parametrically synthesized segments that are simplified counterparts of nineteen bone-segments—five metacarpals, five proximal phalanges, four middle phalanges, and five distal phalanges—of the natural hand-skeleton and simplified mechanical substitutes of the remaining eight carpal bones. 2) A soft skin-like structure that encompasses the artificial skeleton to match the cosmetics and compliant features of the natural hand. A parameterized CAD model representation of each synthesized segment is developed by using the feature of design-tables in SolidWorks, which allows easy customization with respect to each person. Average hand measurements available in the literature are used to

guide the dimensioning of parameters of each synthesized segment. Tendon-driven actuation of the fingers allows the servo actuators to be mounted remotely, thereby enabling a sleek finger design. A prototype of the robotic hand is constructed by 3D-printing all the parts using an Object 30 Prime 3D printer. Results reported from physical validation experiments of the robotic hand demonstrate the feasibility of the proposed design approach.

This thesis is dedicated to my family, especially my dad.

ACKNOWLEDGMENTS

This thesis would not have been successfully complete without the vital contribution of many people. My advisor, Dr. Krishnanand Kaipa, who has always guided me throughout the whole process deserves special recognition. I would like to thank Dr. Sebastian Bawab, the Chair of the MAE Department, for his constant support. I extend many thanks to Dr. Bawab and Dr. Julie Hao, my committee members, for their patience and hours of guidance on my research and editing of this manuscript. A special thanks goes to my lab members Farid Tavakkol, Michael Wang, Parimal Prajapati for their support they offered me during my thesis work. On a personal note, I'd like to thank my mom and my brother for their support and encouragement throughout this endeavor and my father who is showering his blessings on me from heaven.

TABLE OF CONTENTS

LIST OF TABLES

LIST OF FIGURES

CHAPTER 1

INTRODUCTION

1.1 Motivation

"*The hand is a tool of tools…*," is a popular quote by Aristotle. The paramount importance of hands in our lives is reflected in their ability to perform a plethora of manipulation and gestural tasks typical to activities of daily living (ADL). A human hand represents a complex mechanism, with amazing dexterity and utility, and is capable of performing fine manipulation and intricate tasks [13]. In this light, hand loss represents a devastating damage, causing reduction in functionality and incapability to carry out basic manipulation and grasping tasks. Statistics reveals that there exists a high prevalence of population with hand impairments around the world [14]. For example, roughly 541,000 Americans suffered from upper limb loss in 2005, and this number is expected to be doubled by 2050. Around 3500 and 5200 upper limb amputations are reported per year in Italy and in UK, respectively. Approximately, twelve percent of these cases are reported as transradial impairments.

Past solutions to prostheses were mainly passive in nature. Few DOFs (Degree of Freedom) made movement appear unnatural. They were also uncomfortable and heavy to wear. They also led to psychological problems due to lack of a cosmetic look [15, 16]. Research on approaches to replicate nature's complex design of a human hand continues to grow. Recent emergence in robotic prosthetic technologies have resulted in designs that bear some resemblance to the human hand. Unfortunately, none of the existing solutions successfully accomplishes all features in just one design.

Robotic hands can be broadly classified into two types: 1) Robotic grippers used to perform manipulation and grasping operations, typically carried out in industrial tasks where robot's size

and weight do not matter; 2) Robotic prosthesis used to assist people with hand impairments. This necessitates them to look like a human-hand, have same size, have lightweight, and be comfortable to wear. The focus of this thesis is on the second type. Designing a robotic hand that replicates the functionality and cosmetics of a natural hand is not a straightforward task. It requires a thorough study of its morphology, biomechanics, and control aspects. This thereby necessitates combining insights from different interdisciplinary fields, ranging from engineering to neuroscience [17]. The human hand serves as a principal source of biological inspiration for engineers as they attempt to mimic its remarkable features (e.g., flexibility, dexterity, etc.) and design tools/objects that they can be manipulated by the human hand [18]. In the state-of-the-art, there exist no single prosthetic device that fulfills all desired functional tasks, requiring a person to use different devices to perform different tasks [19]. Whereas prosthetic replacements for impaired joints have been progressing rapidly in past few decades, the number of attempts to address the upper extremity have been relatively few, and the results obtained have been inconsistent and less successful [20]. Moreover, making a small change in a previously developed prosthetic hand takes a lot of design iterations and consume a lot of time and money, which has proven to be a big challenge in this field. Another challenge is to design and fit every mechanism required for the prosthetic hand in a limited space similar to a human hand.

The design of a prosthetic hand should always be preceded by finding the feature priorities stated by a specific user. Biddis [21] provided design priorities of prostheses users, which can be used as a basis for designing a robotic hand. The degree of satisfaction of the prosthesis characteristics for users with different prostheses (passive, body-powered, myoelectric) and the importance of the functional role for active and passive prostheses are reported in a study as shown

in Table 1 below [21]. It is clear from this table that in most of the cases, cost and appearance of the prosthesis high priorities over other features like comfort, function, and durability.

One of the needs of the users is that the prosthetic hand should be able to perform basic grasps for daily activities including pointing index finger, power, pinch and lateral grasps. A study of the users revealed that the satisfaction level for comfort, functionality, and appearance were low. The level of anthropomorphism with respect to aspects like shape, size, weight, and color need to be increased in order to enhance acceptability among users. Many prosthetic hands have less number of DOFs as compared to natural human hand, which makes the movement with such prosthetic hands appear unnatural. They appear to be uncomfortable and heavy even with the same weight as a human hand [15, 22].

TABLE 1

Design priorities of passive, body powered, and myoelectric prosthesis (The ranking of

importance is shown in parentheses)

Type of Prostheses	Design Priorities
Passive	Comfort (2.00)
	Appearance (2.46)
	Function (3.06)
	Durability (3.31)
	Cost (4.18)
Body-Powered	Comfort (2.07)
	Appearance (3.89)
	Function (2.07)
	Durability (3.25)
	Cost (3.73)
Myoelectric	Comfort (1.91)
	Appearance (3.01)
	Function (2.39)
	Durability (3.23)
	Cost (4.45)

1.2 Goals and Contributions

This thesis presents the design of a robotic prosthetic hand, which mimics the morphology of a human hand. Its primary goal is to develop a systematic methodology that enables us to

custom-build the prosthesis to match the specific requirements of a person with hand impairments. It addresses two principal research questions toward this goal: 1) How do we cater to the large variation in the distribution of overall hand-sizes in the human population? 2) How closely do we mimic the complex morphological aspects of a biological hand in order to maximize the anthropomorphism (human-like appearance) of the robotic hand, while still maintaining a customizable and manageable design? The design approach attempts to replicate the crucial morphological aspects in the artificial hand (the kinematic structure of the hand skeleton, the shape and aspect ratios of various bone-segments, and ranges of motion). The hand design is partitioned into two parts: 1) A stiff skeleton structure, comprising parametrically synthesized segments that are simplified counterparts of nineteen bone-segments—five metacarpals, five proximal phalanges, four middle phalanges, and five distal phalanges—of the natural hand-skeleton and simplified mechanical substitutes of the remaining eight carpal bones. 2) A soft skin-like structure that encompasses the artificial skeleton to match the cosmetics and compliant features of the natural hand. A parameterized CAD model representation of each synthesized segment is developed by using the feature of design-tables in SolidWorks. This allows easy customization of the dimensions as per the person. Average hand measurements available in the literature are used to guide the dimensioning of parameters of each synthesized segment. Tendon-driven actuation of the fingers allows the servo actuators to be mounted remotely, thereby enabling a sleek palm and finger design. A prototype of the robotic hand is constructed by 3D-printing all the parts using an Object 30 Prime 3D printer. Results reported from different physical validation experiments of the robotic hand demonstrate the feasibility of the proposed design approach.

CHAPTER 2

RELATED WORK

A tremendous amount of work has been done in the field of robotic prostheses till date. Designs ranged from simple passive prostheses to robotic hands, which interface directly with the brain. Few researchers preferred to make the hand under-actuated, while others preferred to make it fully actuated. A general observation in all these anthropomorphic robotic hands is that they resemble close to a human hand. The design focus differs from one robotic hand to another, based on features like cost, fabrication method, weight, speed of finger motion, actuators, under-actuation versus full-actuation, and the number of degrees of freedom used to achieve hand motion.

Developing an anthropomorphic hand needs to go through several stages staring from deciding the size of hand, the number of fingers to incorporate, the degrees of freedom, the range of motion, the method of actuation, and the weight of whole hand. Even with considering these constraints and using an appropriate controller, anthropomorphic robotic hands fail to produce dexterous movements matching a human hand. Sometimes the appropriate actuator cannot be used in the design, as it does not follow the size and weight constraints. The design itself has to go through numerous iterations before actual 3D printing. All these constraints make it difficult to achieve dexterous behavior of hand with several DOF.

Some robotic hands consist of exoskeletons that are designed to improve the performance of human hand in routine tasks. These are used as support in rehabilitation of injured hand or in extravehicular tasks of astronauts. Whereas some robotic hands are designed such that they get benefited from hand-like structure, helping them in reducing the number of end effectors while

performing tasks with several objects [23]. Figure 2.1 shows some of the robotic hands developed previously.

TABLE 2

Previous robotic prosthetic hands

Robotic Hand	No. of Fingers	DOF	No. of Actuators	ROM	Weight (gm)	Actuation/Transmission
Human Hand	5	23	40	-	-	Intrinsic and extrinsic muscles
Vanderbilt Hand (2009)[3]	5	16	5	-	580	Brushed DC Servomotors
Vincent Hand (2010)[16]		6			-	DC Motor-Worm Gear
i-Limb(2009)[2]	4	5		<human hand	443-515	DC motors, belt transmission
DARPA Hand [24]	4	11		<human hand	≈ Human Hand	DC motor, cable, gear transmission
NAIST Hand[7]	4	12	12	≈human hand		geared DC motor, bevel gear (gear driven mechanism)
Robonaut (1999)[6]	5	11	14	≈ Human Hand	1200	DC motor, flex shaft, lead screw, cable
Shadow (2008) [4]	4	17		≈ Human Hand	4200 (Hand and Forearm)	air muscle, cable and spring

Table II (cont.)

|						
Bebionic (2010) [1]	5	6	5	-	550-598	5 DC motors, Lead screw
Michelangelo (2012) [9]	5	2			420	2 DC motors
TCP hand (2017)	5	16	10		-	Tendon-like driven mechanism
DART hand[25]	5	19	19			Electrical motors, Tendon-like driven mechanism
SMA Hand [26]	3	8	9		-	SMA wires
KITECH-Hand (2017) [10]	4	16			900	-
Utah/M.I.T [5]	4	16	38	<human hand	-	Cable, Pneumatic actuator
UB Hand 3[8]	4	15	16	<human hand	-	HiTec Servos
Gifu Hand III [11]	5	16		≈ Human Hand	1400	DC motor, gear transmission, linkage mechanism
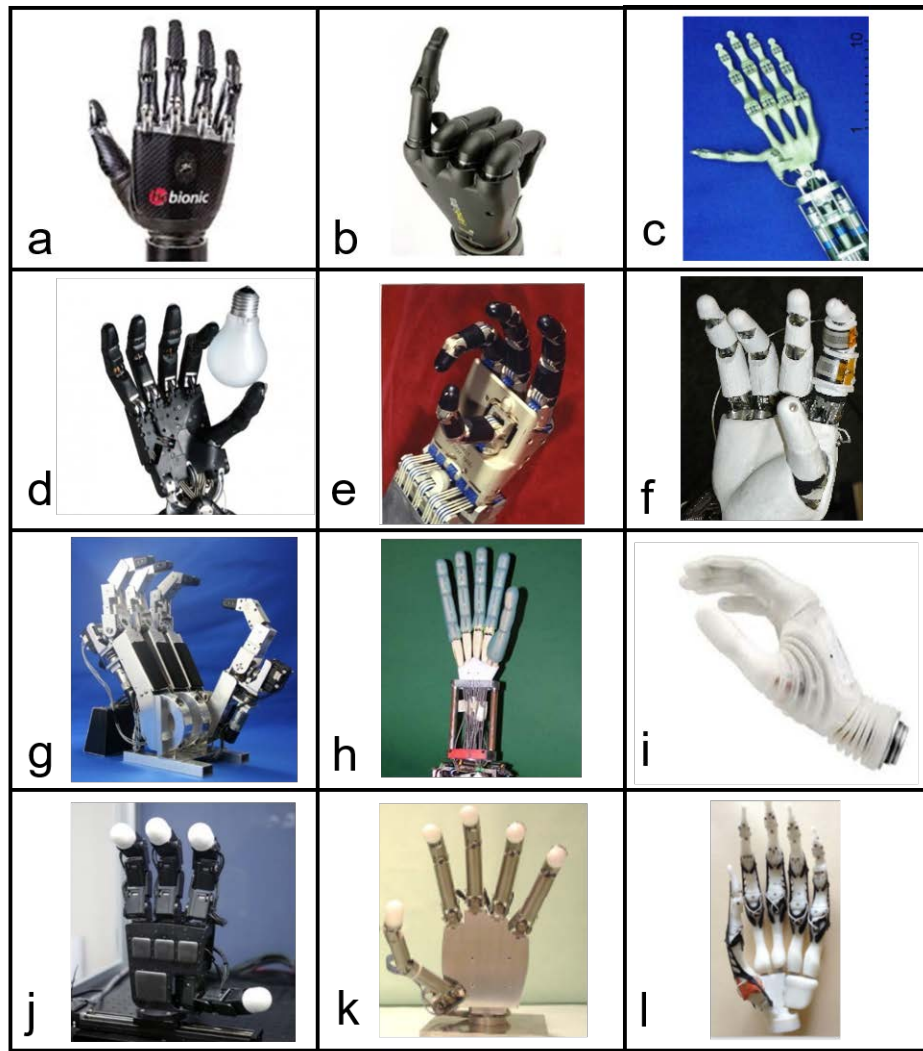
Fig. 2.1. Robotic hands developed in last few years [1-12]

a)   Bebionic, b) i-limb, c) Vanderbilt Hand, d) Shadow Hand, e) Utah/MIT,

f) Robonaut, g) NAIST, h) UB hand 3, i) Michelangelo, j) KITECH- Hand, k) Gifu hand III, l)

University of Washington Hand

2.1 State-of the-art Robotic Prosthetic Hands

The *Bebionic* is a commercially available myoelectric prosthetic arm with four fingers and one thumb. This robotic hand allows freedom of choosing a grip pattern from fourteen available patterns with the help of muscles situated in their forearm, without controlling specific finger separately [1]. It incorporates five high speed/force motors. It is provided with an adjustable thumb to change it from opposed or non-opposed position. The user has to change the position of thumb. All actuators are situated in the palm of the hand. The hand is covered with multilayered silicone gloves with a fabric mesh reinforcement.

The *KITECH-Hand* consists of four fingers. The main attention is on the structure of metacarpophalangeal (MCP) joints of hand, which is roll-pitch type. The unique structure of MCP joint increases the thumb opposability and fingertip manipulability in the common workspace between the thumb and fingers. The design of the MCP joint allows low-cost production by facilitating the modularization. This also improves the dexterity of the robotic hand. The hand shows high dexterity. The KITECH-Hand weighs less than 1 Kg, including inserted electronics. This design is fully actuated with sixteen DOF joints [10].

Amputation can occur at any point of the hand. Placing actuators in the arm or wrist makes it impossible to use the prosthetic hand for patients having their arms and palms intact but missing a few fingers. The *i-Limb* uses a different approach for placement of the actuators. The electric motors are directly placed in prosthetic fingers, making it feasible to use for any kind of hand amputation. A socket is designed in such a way that it incorporates the palm region of hand. All fingers are attached to hand using this socket [2]. Usage of motors to fit in the fingers have the drawback of making the fingers heavy and slow-moving.

Many research teams are focusing on making the hand tendon-driven to make it under-actuated. The *Vanderbilt Hand* makes use of artificial tendons for the finger movements. Brushed DC motors actuate the tendons, making three finger joints to close. The fingers are opened using a spring placed in the finger joints [3]. It uses coiled steel springs for the joints. These springs assist to perform extension movement of fingers without much need of actuation as they store energy during the flexion movement.

A *Shadow Hand* is of size equal to an average human male hand, and is able to perform almost all human hand motions using four fingers and one opposing thumb. Along with these fingers, it also has a palm, a wrist, and a forearm. Each finger incorporates four DOFs, except the pinky finger that has one extra DOF to permit a curling motion of palm. The thumb has five DOFs. However, the approach used by a Shadow Hand to tension the tendons was to use pneumatic air muscles to achieve twenty-four DOFs. This make the design very heavy as it needs a large area for the tendons. This disadvantage of more weight creates difficulty in attaching the hand to an amputee [4, 27].

A four fingered, sixteen DOF, human-hand-sized, anthropomorphic hand was developed by the University of Utah and Massachusetts Institute of Technology [5]. This hand consists of three fingers (ring and pinky fingers are excluded) and a thumb. The hand was designed to perform dynamic manipulation jobs. It incorporates sixteen joints along with tendon and pneumatic piston mechanism. It is able to perform many human hand-like motions. Finger motion is detected by several sensors. The hand is graceful in operation due to impedance of pneumatic actuators. The design contains many couplings among the finger joints and the antagonistic tendons make the whole assembly complex.

To assist space astronauts to perform their duties, NASA developed *Robonaut*, a humanoid robot with a hand comprising fourteen DOFs and resembling an astronaut's hand. It consists of five fingers and a palm. Its palm has a degree of freedom to ease the use of tools. The wrist has two DOFs. The remaining twelve DOFs are present in the hand. Whereas the dexterous work set consists of index, middle, and an opposable thumb, with three DOFs each used for grasping and manipulation, the grasping set consists of ring and pinky finger with one DOF each and a palm DOF [6].

NAIST is another robotic hand that has four fingers with twelve DOFs. Each finger has three DOFs with a distribution of two DOFs at PIP joint (coupled with DIP joint) and one DOF at MP joint. Usage of a three-axis gear mechanism makes the design to work without the use of tendons [7].

The University of Bologna has developed *UB Hand 3*; a humanoid robot whose hand design has anthropomorphic aspects of human hand. It consists of four fingers and one thumb. The hand is covered with a continuous soft cover protecting it from unpredicted forces and impacts from the environment. In order to simplify the mechanical design, it followed an endo-skeletal articulated frame. The compliant features for finger design are made with close-wound helical springs. These springs enable achieving large movements without any deformation or buckling of the spring [8].

The *Michelangelo Hand* has a stiff closure and compliant opening of fingers due to transmission mechanism driving index and middle finger. The fingers comprise of a single finger segment actuated only at a single point similar to the human MCP joint. The thumb has a natural looking rest position. These fingers are made up of linkages with compliant material and pre-loaded cables located at the end of these links [18, 28].

The *GIFU Hand III* consists of a thumb and four fingers. It is actuated by servomotors that are located in the fingers and the palm. In total, it has twenty joints with sixteen DOFs. The thumb has four joints with four DOFs and rest of the fingers have four joints with three DOFs. It has a six-axes force sensor at each fingertip and a developed distributed tactile sensor with 859 detecting points on its surface [11].

The University of Washington has developed a biomimetic anthropomorphic hand. The approach used for the hand is to design artificial joint capsules, crocheted ligaments and tendons, and extensor hood [12]. All bone parts required for the design were 3D printed with available 3D printable files, enabling a high degree of mimicry of natural bones. More than two servos are used for actuating the index finger, the middle finger, and the thumb.

2.2 Actuation Method

There are mainly two types of finger actuation: 1) Fully actuated and 2) Under-actuated. In fully actuated fingers, the number of actuators is equal to DOFs. In underactuated fingers, the number of actuators is less than DOFs. For a mechanical finger, self-adaptability is the best way to define underactuation. With only one actuator and simple control strategies, the object to be grasped is enclosed in these self-adaptive fingers and fingers easily adjust to the shape of an object. To achieve more stable grasps like a human hand, it is desirable to have three phalanges of a finger with three DOFs. This will lead to an effective shape adaption. The working of a finger solely depends on the geometry of the finger design. Geometry is very crucial as all DOFs cannot be controlled independently [29]. All the phalanges of a finger are controlled with just one actuator.

Many tendon-driven robotic hands are being developed these days, which are under-actuated [27, 30-34]. The tendon-driven mechanism enables to reduce the weight of the prosthetic

robotic hand as they can be actuated with very few actuators. The tendon-driven mechanism imitates the muscles and tendon mechanisms of a human hand. The use of tendons not only allows to reduce the weight, but also gives the benefit of being flexible and back-drivable. More flexibility of finger movement is achieved through the help of tendon-driven mechanism. Plentiful efforts have been put in developing a tendon-driven mechanism for a humanoid robotic hand, but still the dexterity of a natural human being is yet to be achieved.

Usually, the tendons have to be stiff to achieve full movement of all fingers. Many researchers have suggested incorporating elasticity into robotic actuators. This improves the precision and stability and reduces the end-point position error under load disturbances [35]. The mechanism includes the spring in series with a stiff actuator. Compliance is fixed during the operation as it depends upon the spring constant [36].

CHAPTER 3

DESIGN METHODOLOGY

The design approach in this thesis attempts to replicate the crucial morphological aspects in the artificial hand (the kinematic structure of the hand skeleton, the shape and aspect ratios of various bone-segments, and ranges of motion). The hand design is partitioned into two parts: 1) A stiff skeleton structure, comprising parametrically synthesized segments that are simplified counterparts of natural bone-segments, and 2) A soft skin-like structure that encompasses the artificial skeleton to match the cosmetics and compliant features of the natural hand. A parameterized CAD model representation of each synthesized segment is developed by using the feature of design-tables in SolidWorks, which allows easy customization with respect to each person. Average hand measurements available in the literature are used to guide the dimensioning of parameters of each synthesized segment. Tendon-driven actuation of the fingers allows the servo actuators to be mounted remotely, thereby enabling a sleek finger design. A prototype of the robotic hand is constructed by 3D-printing all the parts using an Object 30 Prime 3D printer.

3.1 Biological Inspiration: Natural Hand Morphology

Studied and presented here are the anatomical details of the human hand to capture the morphological aspects that are crucial to the basic functionality of the hand. A hand's dexterity is recognized by its near about twenty DOFs [37]. The thumb is the most independent among all the five digits of the hand [38] and it differs in terms of kinematics, size, and strength of its muscles [39]. The distribution of DOFs among the fingers is same except the thumb. Each finger

has four DOFs, three for flexion/ extension and one for abduction/adduction at CMC joint, while the thumb has 5 DOFs. Figure 3.1(a) shows the dorsal view of a human right hand comprising cross-section of the little finger, dissection of the ring and middle fingers, and the radiography of thumb.
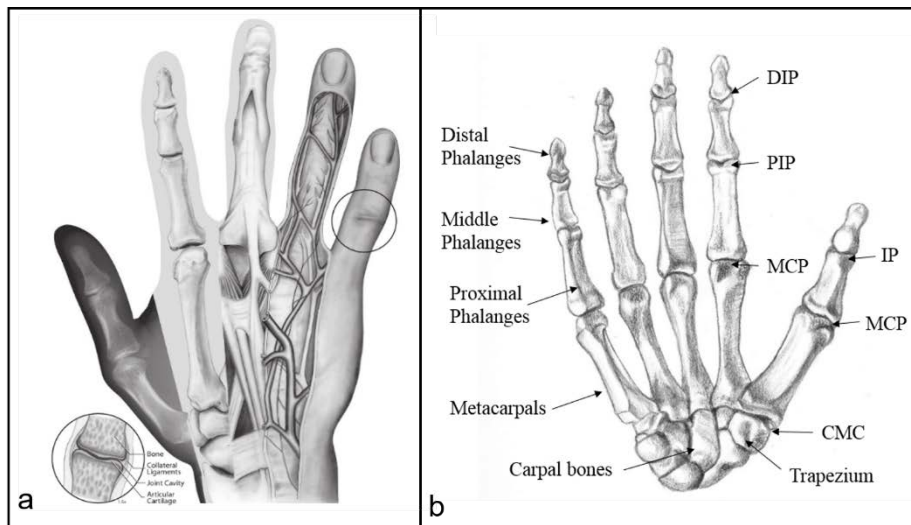
Fig. 3.1. (a) Human right hand (Dorsal view). Includes cross-section of little finger, dissection of ring and middle finger and radiography of thumb. [40] (b) Human hand skeletal structure depicting finger bones, joints, metacarpals, and carpal bones.

3.1.1 Bones and Joints

The human hand is very complex in structure. It consists of overall twenty-seven bones comprising eight carpal bones, five metacarpal bones of palm region, and fourteen phalange bones in the digits of hand. The phalangeal bones are not evenly distributed in all digits. The thumb has two phalanges, while the remaining digits have three phalanges each. The eight carpal bones are organized in two rows. The proximal row consists of scaphoid, lunate, triquetrum, and pisiform.

The distal row consists of trapezium, trapezoid, capitate, and hamate. The distal row articulates with metacarpals of all fingers. The metacarpal bones articulate with the carpal bones, forming carpometacarpal joints helping flexion/extension along with a deviation of radial and ulnar. With very limited independent motion of these joints, there is an increment in the range of motion from the second through fifth metacarpals. However, the thumb is an exception for this. All the nine interphalangeal joints in the fingers have only flexion and extension movement. Each finger has three bones, the proximal, middle, and distal phalanges. Depending on the placement of joint, these joints are called as metacarpophalangeal (MP), the proximal interphalangeal (PIP), and the distal interphalangeal (DIP) joint [41]. Figure 3.1(b) shows the bone structure of a human hand.

The thumb has an unique capability to oppose other four fingers. A larger set of bones are involved in the opposition mechanism (Figure 3.1(b)), like the trapezium, the trapezoid, and the scaphoid [39]. Unlike other digits, the thumb does not have a middle phalanx. Therefore, with only two phalanges it has better mobility for carpometacarpal joint as compared to the remaining digits. The thumb has two DOF at the carpometacarpal joint.
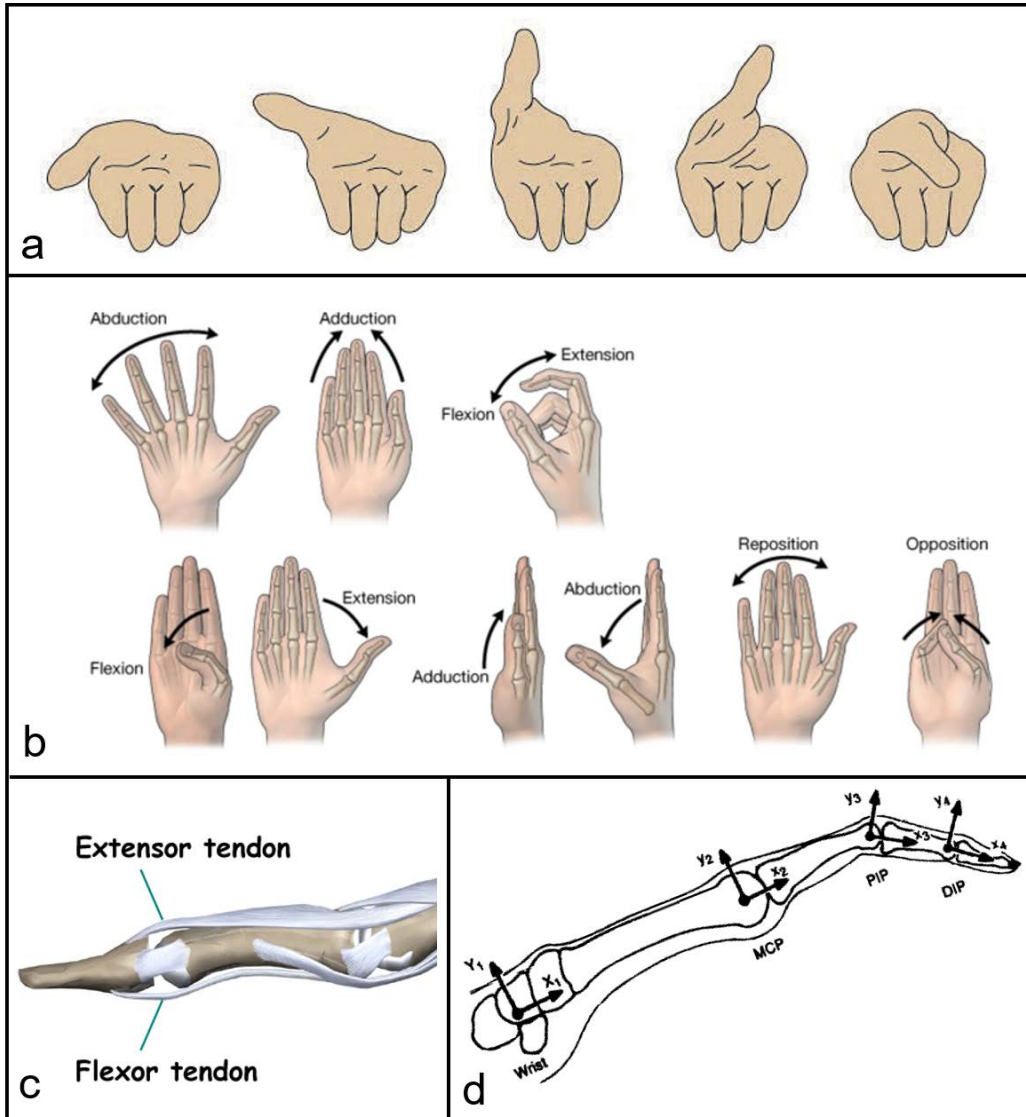
Fig. 3.2 (a) Schematic drawing showing the range of motion of thumb's CMC joint ranging from Full extension (left) to full extension (right) [42], (b) Diagram showing finger movements of digits index, middle, ring and pinky, and thumb movement [43], (c) Musculotendinous structure of a long finger, (d) Kinematic skeleton of human hand [44]

Along with the flexion/extension and abduction/adduction movement, the thumb has significant axial rotation. This movement is not taken as a third DOF of a thumb because this

motion is constrained [41]. In a human hand, the nine interphalangeal joints (PIP, DIP, and IP) are termed as hinge joints and the five MCP joints are termed as saddle joints. Whereas the hinge joints are capable of only flexion and extension, the saddle joints have an extra motion known as abduction/adduction. The CMC joint of thumb is termed as saddle joint with two DOFs. Due to incongruity between the metacarpal and the trapezium bone of thumb, the metacarpal of thumb has a significant rotation [44]. The critical component responsible for the opposition movement is the trapezium bone situated at the base of thumb. The CMC joint is considered as a saddle joint allowing wide range of motion, because of unique shape of trapezium bone. These motions include up (adduction) and down (abduction), bent (flexion) and straightened (extension), and the ability to move through the palm (opposition) (Figure 3.2).

3.1.2 Tendons

Tendons and muscles cover the joints between each phalanx [45]. These are the tough cords of tissue creating link between muscles to bones [46]. Bony and ligamentous guide systems have a way for tendons and muscles to pass (Figure 3.2(c)). Generally, the tendons are divided in two groups depending on the motion of contraction. Extensor tendons run from the forearm and back of hand to fingers and thumb, and aid in straightening the fingers. Flexor tendons run from the forearm, through the wrist and across the palm, and aid in bending the fingers. The greater multangular, carpal bones, the projection of the hamate, and the tough transverse carpal ligament create a way for the passage of flexor tendons. The dorsal carpal ligament guides the extensor tendons, and flexor and extensor tendons get passage through sheaths through the metacarpal and phalangeal area [13].

The important function of tendons is to trigger motion by transferring force from muscle to bone. The muscles and the actuators can be compared with a mechanical system where muscles

serve the purpose of an actuator for generating the forces, while tendons can be treated as the transmission system with the purpose of dividing forces, along with transmitting torques to every finger joint. Tendons have the capacity to withstand high tensile forces caused due to muscle contraction taking place in joint movement [47].

3.2 Translation from Natural to Synthetic Hand

Designing a robotic hand that closely mimics a natural hand requires an appropriate translation of the crucial morphological features from the natural hand to the synthetic hand. These features include the kinematic structure of the hand skeleton, the shape and aspect ratios of various bone-segments, and ranges of motion. Emphasis is on maximizing the anthropomorphism, while still maintaining a customizable and manageable design. This is achieved by incorporating the following translation procedure into the synthetic hand design:

1) Nineteen out of twenty-seven bones are replicated. These bones include five metacarpals, five proximal phalanges, four middle phalanges, and five distal phalanges.

2) Remaining eight carpal bones are approximated by two synthetic segments in the wrist.

3) The average aspect-ratios of a natural hand are maintained throughout all the bone segments of the synthetic hand.

4) The complex shape of each bone-segment is simplified by synthetic segment with varying circular-cross section.

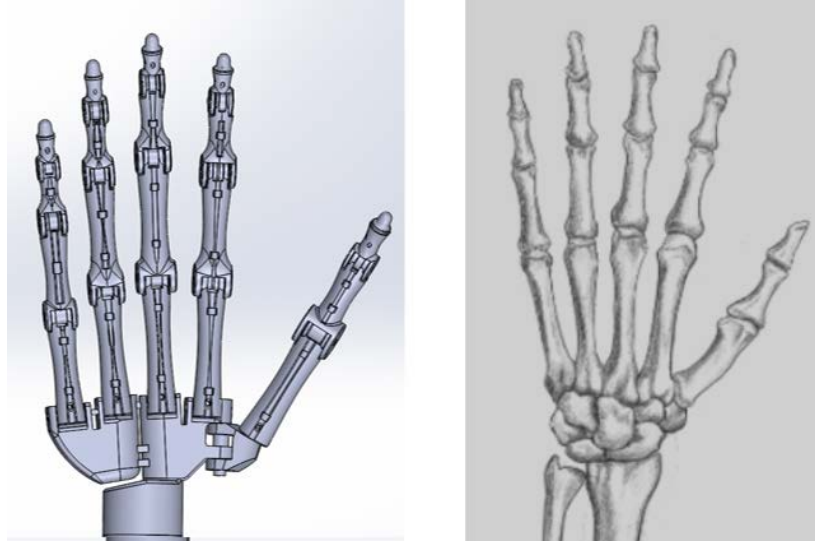5) Hinge-joints of all phalanges are simplified by pin-joints.

Fig. 3.3 Diagram showing resemblance between the design and human hand skeleton

3.3 Kinematics

Kinematics is the science of motion that treats the subject without concern of the forces that cause it. It involves the study of motion including position, velocity, acceleration, and other higher order derivatives of position. In short, it refers to all geometrical and time-based properties [48]. Degree-of-freedom (DOF) of a mechanical system is defined as the minimum number of independent variables required to describe its configuration completely. Kinematics of the hand is a function of the number of DOF and the degree of control as per the requirement of goal to be achieved. A human hand's kinematics is driven by very a complex muscle-tendon system. Replicating all the ranges of movements that a human hand can produce is very challenging due to the constraint that all the mechanical components required for the movement must be placed inside the finger structure consisting of a limited volume.

This part of thesis will explain the kinematics of all four fingers and thumb. All fingers (index, middle, ring, and pinky) have four links with three DOFs. However, the thumb has three links with four DOFs. The design for the finger has three joints imitating the DIP, PIP, and MCP.

Each joint has one DOF. The thumb has a different configuration where the IP, MCP, and CMC joint has two DOFs. The base of metacarpal of each finger is fixed at its base. Considering these differences in configurations, two separate kinematic models have been developed.

The kinematic skeleton of the human hand is mathematically represented by joints connected by simple line segments. The nine interphalangeal joints of a human hand, capable of flexion and extension are considered as hinge joints, while the remaining five metacarpophalangeal joints (MCP) are considered as saddle joints capable of both flexion-extension and abduction-adduction motions [44].

Figure 3.4 shows the kinematic model of the synthetic hand. The index, middle, ring, and pinky fingers have four links each, while the thumb has only three links. The kinematic model of each finger consists of four links and four joints. This requires four local moving-frames, assigned one at each joint, and a local fixed-frame assigned at the base of its metacarpal bone. Similarly, the kinematic model of the thumb consists of three links and three joints. This requires three local moving-frames, assigned one at each joint, and a local fixed-frame assigned at the base of its metacarpal bone. A global fixed-frame for the whole hand is assigned at the center of the wrist.
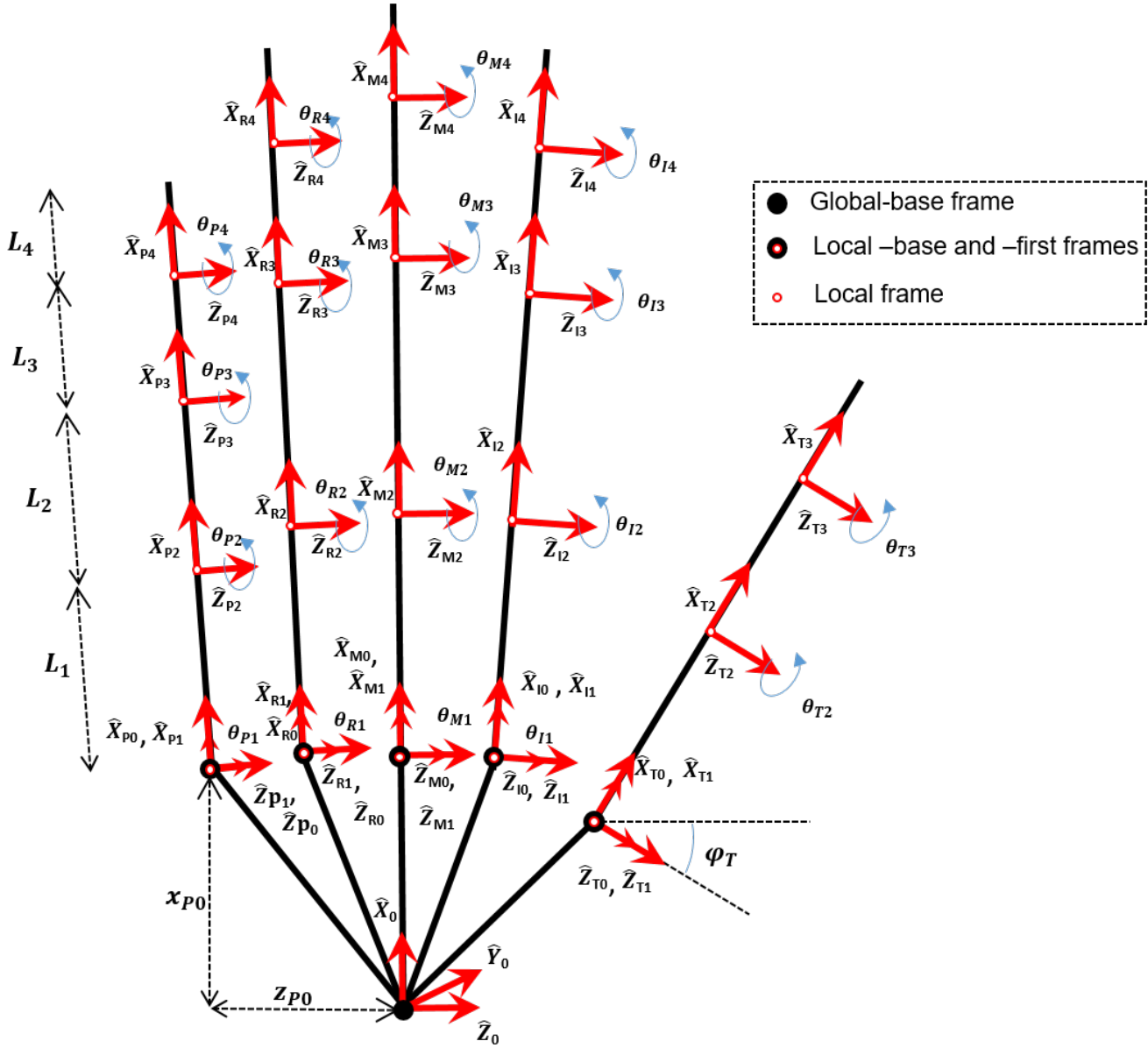
Fig. 3.4. Kinematics of the hand. Fingers are represented by subscript (thumb-T, index-I, middle-M, ring-R, and pinky-P)

3.3.1 Kinematic relationships using D-H parameters

Denavit–Hartenberg parameters, also known as D-H parameters, are used to describe the kinematic relationships between the links. Four parameters are necessary to fully define the pose

of a link relative to its predecessor. According to this convention, these four parameters associated

with link *i* and joint *i* include joint-angle $\boldsymbol{\theta_i}$, link-length $\boldsymbol{a_i}$, link-offset $\boldsymbol{d_i}$, and link-twist $\boldsymbol{\alpha_i}$. The

D-H parameters for the index finger are shown in Table 4. Figure 3.4. shows that the finger has

five frames with four joints. The first frame also known as the base frame is $\boldsymbol{X_0}$, $\boldsymbol{Y_0}$, $\boldsymbol{Z_0}$ and the

subsequent frames are assigned as per the figure starting with $\boldsymbol{X_1}$, $\boldsymbol{Y_1}$, $\boldsymbol{Z_1}$ and ending with $\boldsymbol{X_4}$,

$\boldsymbol{Y_4}$, $\boldsymbol{Z_4}$. The forward kinematic solution of a finger will be assigned using a homogenous

transformation matrix $^{i-1}_iT$ from frame *i* to frame *i-1*:

$$^{i-1}_iT = \begin{bmatrix} cos\theta i & -sin\,\theta i & 0 & ai-1 \\ sin\,\theta i.\cos(\alpha i-1) & cos\theta i.\cos(\alpha i-1) & -\sin(\alpha i-1) & -\sin(\alpha i-1)di \\ sin\,\theta i.\sin(\alpha i-1) & cos\,\theta i.\sin(\alpha i-1) & \cos(\alpha i-1) & \cos(\alpha i-1)\,di \\ 0 & 0 & 0 & 1 \end{bmatrix} \quad (3.1)$$

TABLE 3

D-H PARAMETERS CORRESPONDING TO THE INDEX FINGER

Finger	Frame	α_{i-1}	a_{i-1}	d_i	θ_i
Index	1	0	L_1	0	θ_{I1}
	2	0	L_2	0	θ_{I2}
	3	0	L_3	0	θ_{I3}
	4	0	L_4	0	θ_{I4}

The transformation matrices for the kinematic analysis of the index finger are given below:

$$^{I0}_{I1}T = \begin{bmatrix} cos\theta_1 & -sin\theta_1 & 0 & L_1 \\ sin\theta_1 & cos\theta_1 & 0 & 0 \\ 0 & 0 & 1 & 0 \\ 0 & 0 & 0 & 1 \end{bmatrix} \quad (3.2)$$

$$
{}^{I1}_{I2}T = \begin{bmatrix} cos\theta_2 & -sin\theta_2 & 0 & L_2 \\ sin\theta_2 & cos\theta_2 & 0 & 0 \\ 0 & 0 & 1 & 0 \\ 0 & 0 & 0 & 1 \end{bmatrix} \tag{3.3}
$$

$$
{}^{I2}_{I3}T = \begin{bmatrix} cos\theta_3 & -sin\theta_3 & 0 & L_3 \\ sin\theta_3 & cos\theta_3 & 0 & 0 \\ 0 & 0 & 1 & 0 \\ 0 & 0 & 0 & 1 \end{bmatrix} \tag{3.4}
$$

$$
{}^{I3}_{I4}T = \begin{bmatrix} cos\theta_4 & -sin\theta_4 & 0 & L_4 \\ sin\theta_4 & cos\theta_4 & 0 & 0 \\ 0 & 0 & 1 & 0 \\ 0 & 0 & 0 & 1 \end{bmatrix} \tag{3.5}
$$

Transformation from the local base-frame of each finger to the global base-frame of the hand is as given as below. Values of angles $\varphi_I, \varphi_R \ and \ \varphi_P$ are found out to be 8°, 6°, and 10.22° respectively. As the global base-frame is collinear to the local base-frame of the middle finger, we have

$$
{}^{0}_{M0}T = \begin{bmatrix} 1 & 0 & 0 & 49.28 \\ 0 & 1 & 0 & 0 \\ 0 & 0 & 1 & 8.29 \\ 0 & 0 & 0 & 1 \end{bmatrix} \tag{3.6}
$$

The local base-frames of index, ring, and pinky fingers and the thumb involve both translation and rotation relative to the global base-frame. Therefore, we have

$$
{}^{0}_{I0}T = \begin{bmatrix} \cos(-\varphi_I) & 0 & \sin(-\varphi_I) & 47.19 \\ 0 & 1 & 0 & 0 \\ -\sin(-\varphi_I) & 0 & \cos(-\varphi_I) & 27.27 \\ 0 & 0 & 0 & 1 \end{bmatrix} \tag{3.7}
$$

$$= \begin{bmatrix} \cos(-8) & 0 & \sin(-8) & 47.19 \\ 0 & 1 & 0 & 0 \\ -\sin(-8) & 0 & \cos(-8) & 27.27 \\ 0 & 0 & 0 & 1 \end{bmatrix}$$

$$= \begin{bmatrix} 0.9902 & 0 & -0.13917 & 47.19 \\ 0 & 1 & 0 & 0 \\ 0.13917 & 0 & 0.9902 & 27.27 \\ 0 & 0 & 0 & 1 \end{bmatrix} \tag{3.8}$$

$$_{R0}^{0}T = \begin{bmatrix} \cos(\varphi_R) & 0 & \sin(\varphi_R) & 49.89 \\ 0 & 1 & 0 & 0 \\ -\sin(\varphi_R) & 0 & \cos(\varphi_R) & -8.94 \\ 0 & 0 & 0 & 1 \end{bmatrix} \tag{3.9}$$

$$= \begin{bmatrix} \cos(6) & 0 & \sin(6) & 49.89 \\ 0 & 1 & 0 & 0 \\ -\sin(6) & 0 & \cos(6) & -8.94 \\ 0 & 0 & 0 & 1 \end{bmatrix}$$

$$= \begin{bmatrix} 0.9945 & 0 & 0.1045 & 49.89 \\ 0 & 1 & 0 & 0 \\ -0.1045 & 0 & 0.9945 & -8.94 \\ 0 & 0 & 0 & 1 \end{bmatrix}$$

$$_{P0}^{0}T = \begin{bmatrix} \cos(\varphi_P) & 0 & \sin(\varphi_P) & 46.37 \\ 0 & 1 & 0 & 0 \\ -\sin(\varphi_P) & 0 & \cos(\varphi_P) & -30.56 \\ 0 & 0 & 0 & 1 \end{bmatrix} \tag{3.10}$$

$$= \begin{bmatrix} \cos(10.22) & 0 & \sin(10.22) & 46.37 \\ 0 & 1 & 0 & 0 \\ -\sin(10.22) & 0 & \cos(10.22) & -30.56 \\ 0 & 0 & 0 & 1 \end{bmatrix}$$

$$= \begin{bmatrix} 0.9841 & 0 & 0.1774 & 46.37 \\ 0 & 1 & 0 & 0 \\ -0.1774 & 0 & 0.9841 & -30.56 \\ 0 & 0 & 0 & 1 \end{bmatrix}$$

$$\begin{array}{rl} {}_{T0}^{0}T = & \begin{bmatrix} \cos(30) & 0 & -\sin(30) & 31.46 \\ 0 & 1 & 0 & 0 \\ \sin(30) & 0 & \cos(30) & 48.19 \\ 0 & 0 & 0 & 1 \end{bmatrix} \end{array}$$ (3.11)

$$= \begin{bmatrix} 0.1542 & 0 & -0.5 & 31.46 \\ 0 & 1 & 0 & 0 \\ 0.5 & 0 & 0.1542 & 48.19 \\ 0 & 0 & 0 & 1 \end{bmatrix}$$

3.4 Skeleton Structure using a Parametric Representation

In order to cater to the large variation in the distribution of overall hand sizes in the human population, a parametric representation is used to design the CAD model of each segment of the skeleton structure. Parametrization is crucial for this design as the aim is to serve humans with different hand sizes. However, there will be some features in the design that need to be fixed in dimensions, no matter the hand size. These parameters include pin-size, the diameter of holes for these pins, and the wall-thickness of the parts. The purpose will not be served by simply scaling (up or down) the original model of finger parts. The design table feature of Solidworks can be used to implement such a parametric representation. In particular, a design table allows for multiple configurations of parts by stating parameters with the help of an embedded Microsoft Excel worksheet. The number of parameters to be changed can be easily controlled using the design table.
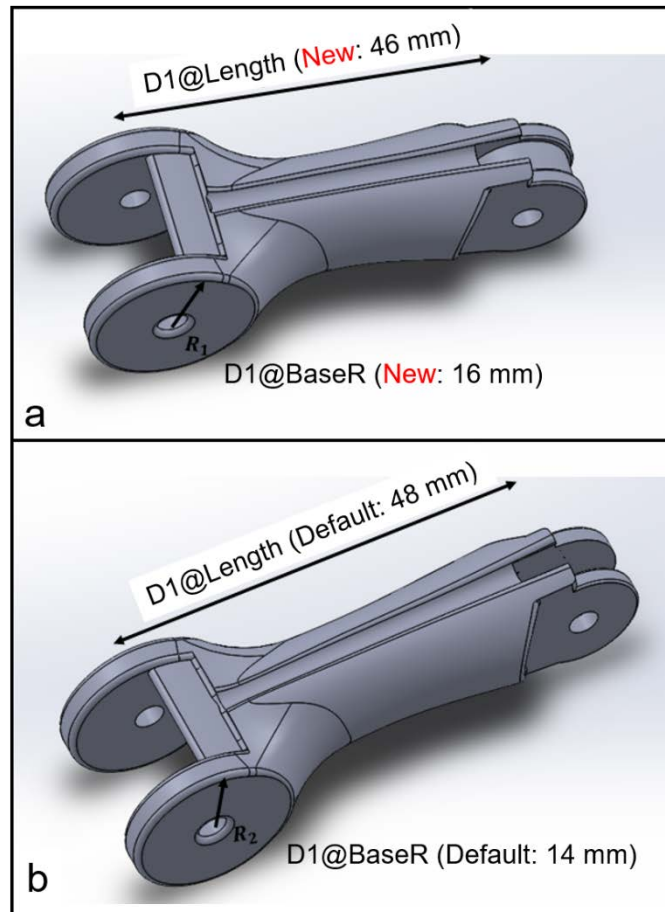
Fig. 3.5. (a) Diagram showing use of design table for configuration change (b) Schematics of
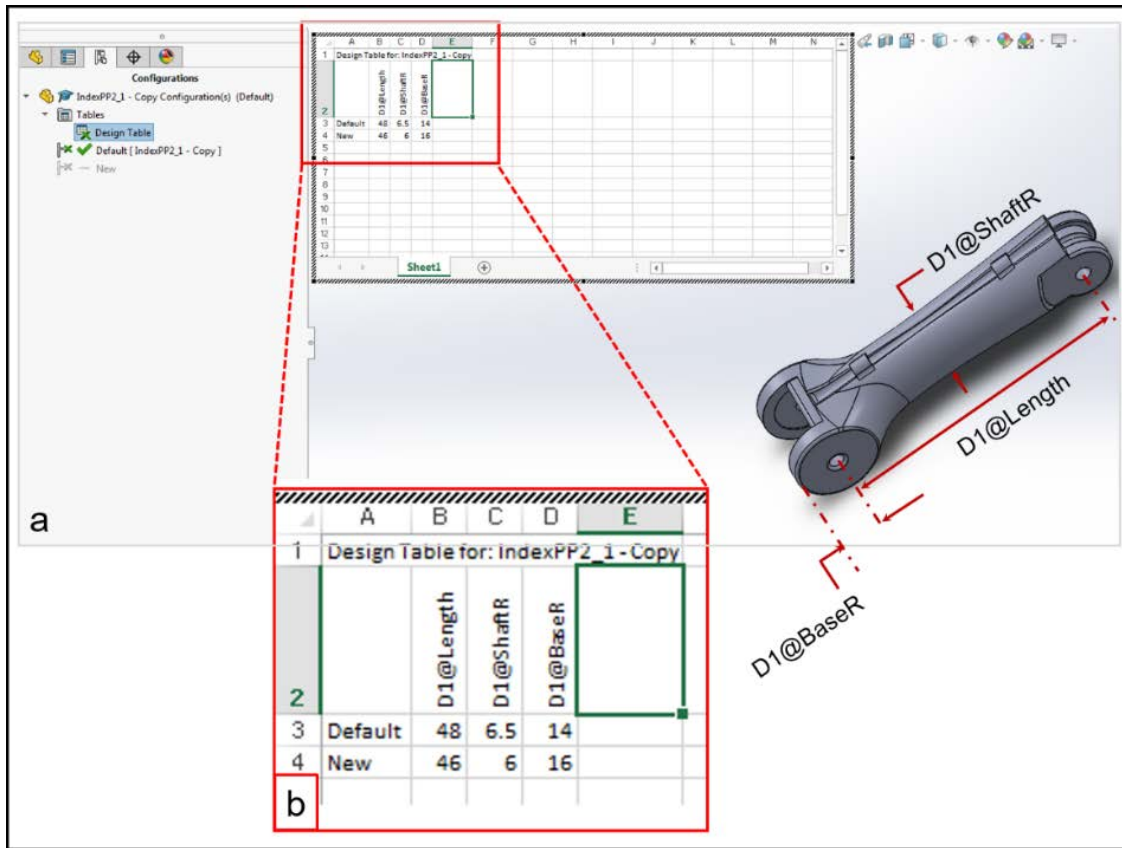
design table

Fig. 3.6. Two different configuration of the same part

Figure 3.5 illustrates the design table feature. Figure 3.5 (a) shows the two configurations of an index middle phalange with just five parameters to change. Figure 3.6 shows the two different configurations of the same bone part with different lengths. These design tables were used to get the new configuration of another hand. Examples of average hand measurements from the literature are shown in Table 4.

TABLE 4

Parametrized configuration (A: Length of bone, B: Shaft radius, C: Base) (in mm)

Fingers		Distal Phalanx			Middle Phalanx			Proximal Phalanx			Metacarpal bone		
		A	B	C	A	B	C	A	B	C	A	B	C
Index	Subject 1	22	5.25	10	31	9.54	14	58	10.93	19	78	11.76	20
	Subject 2	20.64	5.2	15.38	26.12	9.22	13.67	46.24	10.03	16	52.17	11.58	18.43
Middle	Subject 1	23	11.34	10	39.75	12.16	18.48	64.93	13.34	22.53	78.8	13.96	20
	Subject 2	21.94	11.09	13.60	31.12	12.14	16.06	48.74	13.21	17.74	57.15	13.89	18.55
Ring	Subject 1	22.40	5.22	10.71	29.25	9.10	13.62	55.58	11.03	18.85	70.03	10.31	19
	Subject 2	22.22	5.2	10.29	21.61	8.64	12.40	44.11	9.90	16.80	51.41	9.97	17.12
Pinky	Subject 1	22.44	5.05	10.91	24.63	7.74	11.47	44.47	8.91	15.41	68	11.08	13.4
	Subject 2	17.68	5.69	8.89	20.11	8.07	10.22	33.20	10.74	13.93	48.56	10.80	13.29
Thumb	Subject 1	28.76	8.11	10.02	-	-	-	39.56	11.54	19.68	64.22	15.40	20.54
	Subject 2	26.24	9.88	10.73	-	-	-	36.78	12	19.16	55.34	15.01	18.37

Using the dimensions above, the index finger has been reproduced with new dimensions of other hand. Using the same method, other parts of the design can be changed based on a new configuration (see Figure 3.7).
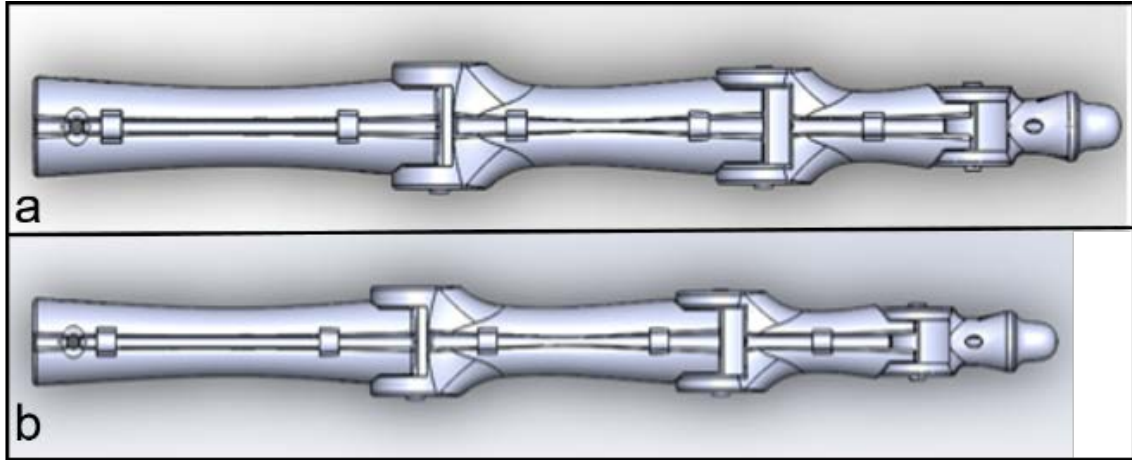
Fig. 3.7. Index finger a: Original configuration b: New configuration

3.5 Lessons Learned from 3D printing of Open Source Robotic Hand

It is not possible to place a servomotor at each DOF of the finger due to size restriction. As a solution, these fingers need to be actuated remotely with a single servo per finger. This can be achieved by using a tendon-driven mechanism, in which a tendon (cable) passes over each finger joint so that the finger is actuated with the help of only one servomotor. Before proceeding with the design, it was necessary to familiarize the tendon-driven mechanisms by 3D-printing and assembling an artificial hand, which was available as a part of 'InMoov', an open source, life-size, humanoid robot [49]. All CAD models needed for the hand were available on the open source site as '.stl' files.

Each finger consisted of six different parts and the palm area was divided into three parts. The palm area beneath the ring finger and pinky finger were designed separately to compensate for the movement of the metacarpal bones present in the palm. The range of motion for metacarpal bones varies from finger to finger. It is less for the index and middle fingers, while it is greater for ring and pinky fingers. Figure 3.8(a) shows the hand design of the InMoov Robot. Figure 3.8(b)

shows the assembled robotic hand and 3.8(c) shows the InMoov robot structure from the trunk and above.
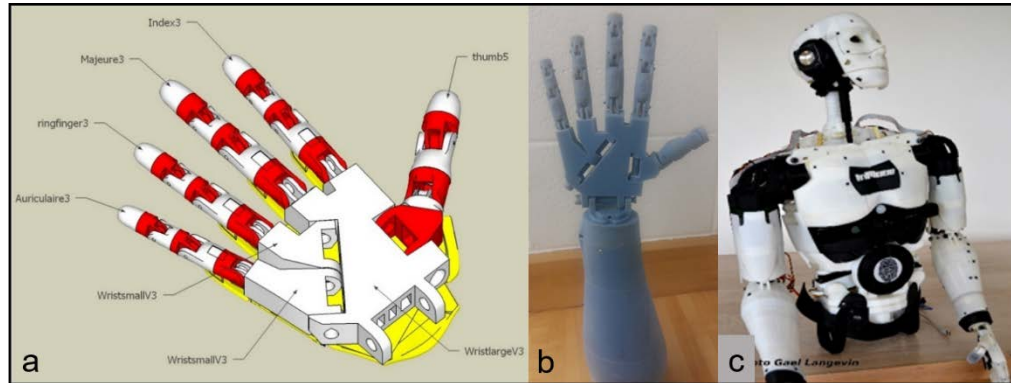

Fig. 3.8. (a) InMoov hand design (b) 3d printed right hand (c) InMoov robot

The whole process of 3D-printing and assembling the robotic hand parts was a great learning experience. It eased the job of designing anthropomorphic hand using tendon-driven mechanisms. The idea of tendon-routing throughout the hand structure became very clear by going through this experience.

CHAPTER 4

SYNTHETIC ROBOTIC HAND DESIGN

The synthetic hand design is partitioned into two parts: 1) A stiff skeleton structure, comprised of parametrically synthesized segments that are simplified counterparts of nineteen bone-segments—five metacarpals, five proximal phalanges, four middle phalanges, and five distal phalanges—of the natural hand-skeleton and simplified mechanical substitutes of the remaining eight carpal bones; 2) A soft skin-like structure that encompasses the artificial skeleton to match the cosmetics and compliant features of the natural hand. As mentioned in Section 3.4, a parameterized CAD model representation of each synthesized segment was developed by using the feature of design-tables in SolidWorks, which allows for easy customization with respect to each person. The average human hand's dimensions available in the literature were used for dimensioning of parameters of each synthesized segment. The design underwent several iterations throughout the process before coming up with the final version. The final design consisted of four fingers (index, middle, ring, and pinky), a thumb, and a wrist. Each finger was subdivided into four segments, representing three phalanges and one metacarpal bone. The thumb was subdivided into three segments, representing two phalanges and one metacarpal bone.

As mentioned in Section 3.5, tendon-driven actuation of the fingers is used to allow the servo actuators to be mounted remotely, thereby enabling a sleek finger design. Basically, there are two tendons for each finger: one tendon runs on the back-side (palmar region) of the finger, enabling its extension, while the other tendon runs on front-side (dorsal region) of the finger, enabling its flexion. A spring is connected in series with each tendon to achieve compliance in the finger movements. The servomotors used are geared DC motors, which can be rotated to a

specified angle in a controlled way. There were totally five servo motors used, one for each finger. A good choice for the tendons was a high quality braided fishing line as it has good resistance to stretching that occurs over the period of time of usage.

4.1 Fingers

Each finger consists of four segments representing metacarpal bone, proximal phalanx, middle phalanx, and distal phalanx. Pins were designed to form a joint between two adjacent segments. Figure 4.1 shows the schematics of a finger along with the tendon route. Artificial tendons pass over the bone segments through a guideway. For each finger, there are two channels for tendons, one from palmar region of finger for the flexion movement, while the other one is at the dorsal side to accommodate the extension movement of finger. The range of movement of each finger is restricted by using a sleeve designed for each finger segment (See Fig. 4.1).
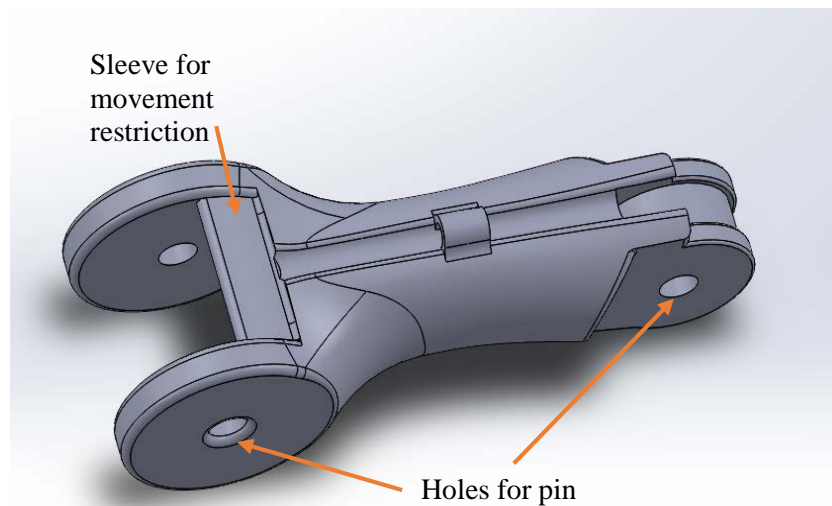

Fig. 4.1. Middle phalanx of an index showing arrangement for movement restriction

Figure 4.2 illustrates the natural finger bones of an index finger and those of synthetic finger bones of this design.
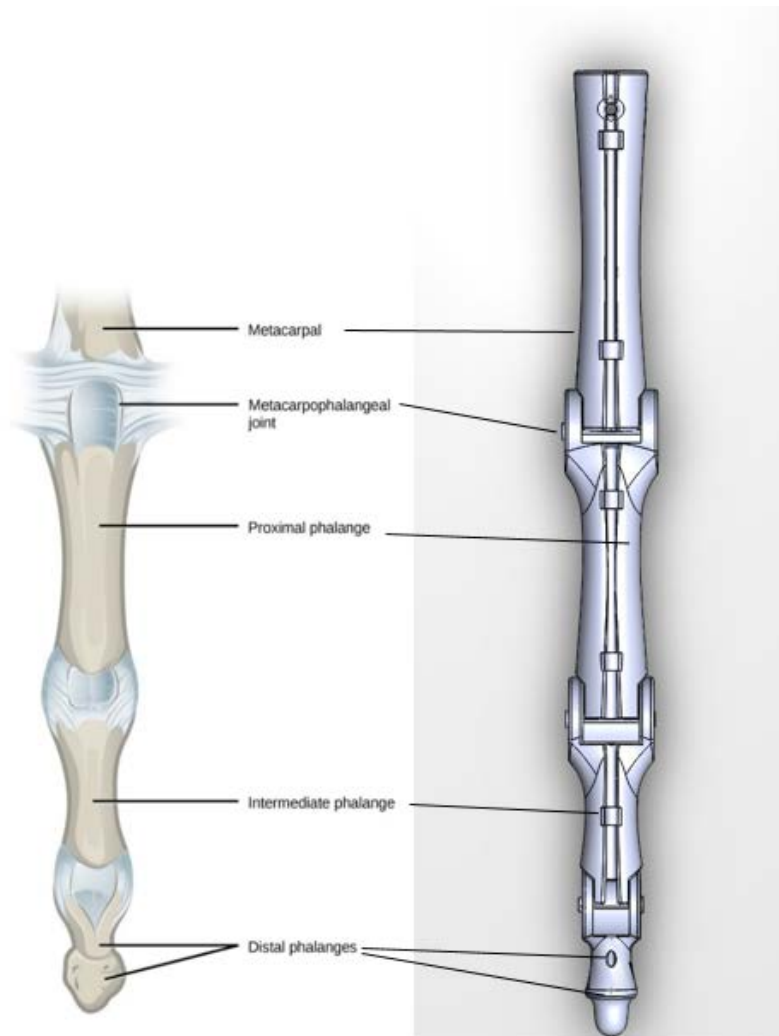

Fig. 4.2. Comparison between the natural finger and the synthetic finger

Tendon routing at the distal phalanx and metacarpal of each finger is from within the bone structure and a knot is tied using the two opposite tendons of the finger.
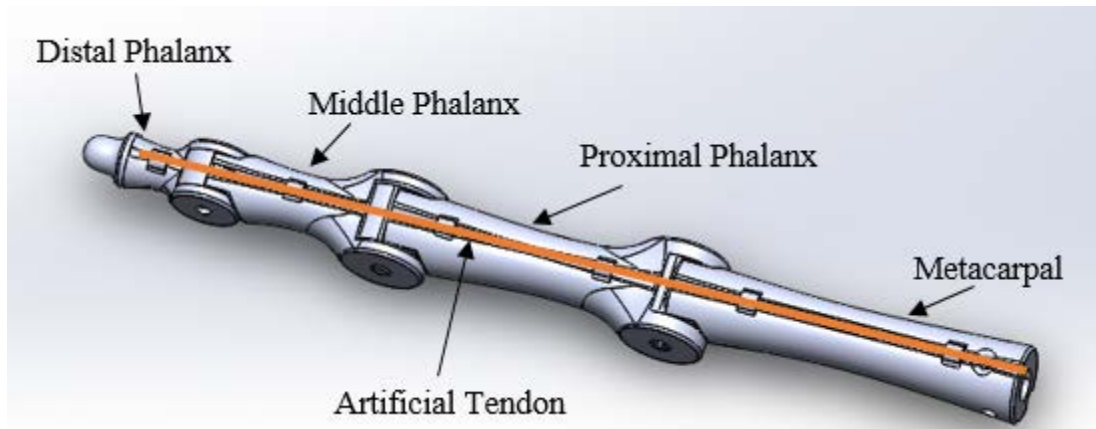

Fig. 4.3. Tendon Route of an Index Finger

4.3 Thumb

The thumb is designed differently from the remaining fingers. Even though thumb only has three bones, the design of thumb was divided into three segments, representing the metacarpal, the proximal phalanx, and the distal phalanx. This design allowed for a thumb with two DOFs, which permitted flexion/extension and abduction/adduction. Tendon-routing is similar to that of the rest of the fingers.
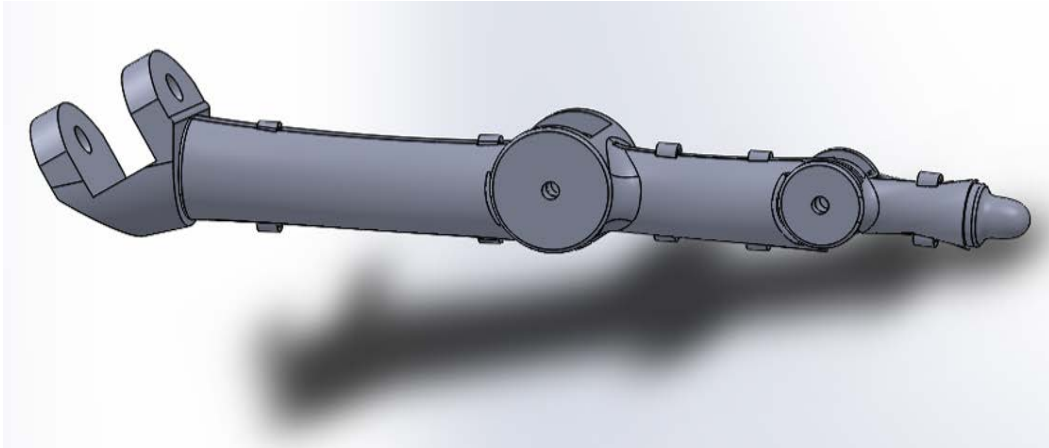
Fig. 4.4. CAD model of a Thumb

4.4 Carpal Bone Segments

The eight metacarpal bones of the wrist have been simplified by two segments of the wrist. The first segment attaches to the metacarpal bones of the index finger, the middle finger, and the thumb. The second segment attaches to the metacarpal bones of the ring and pinky fingers, which have some rotation as it occurs in the natural hand (movement restriction of the metacarpal bone). Figure 4.5(a) shows the wrist assembly. The tendons are routed from inside the wrist as shown in Fig. 4.5(b).
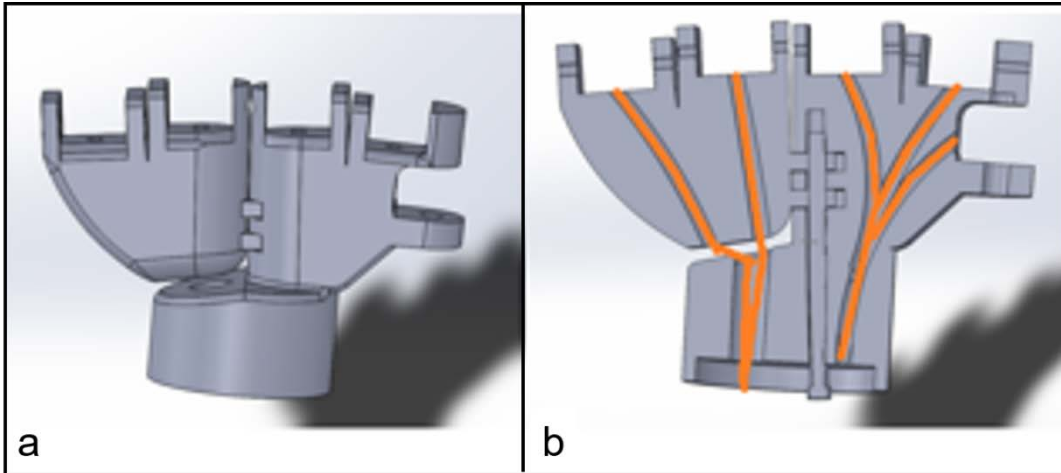
Fig. 4.5. (a) Wrist assembly (b) Section view showing tendon route

4.5 Tensioner

The tensioner is designed for maintaining essential tension in both tendons of a finger. Height of the tensioner is adjustable with the help of screw and nut. The design needs five tensioners, one for each finger that are placed on the forearm of hand (Fig. 4.7).
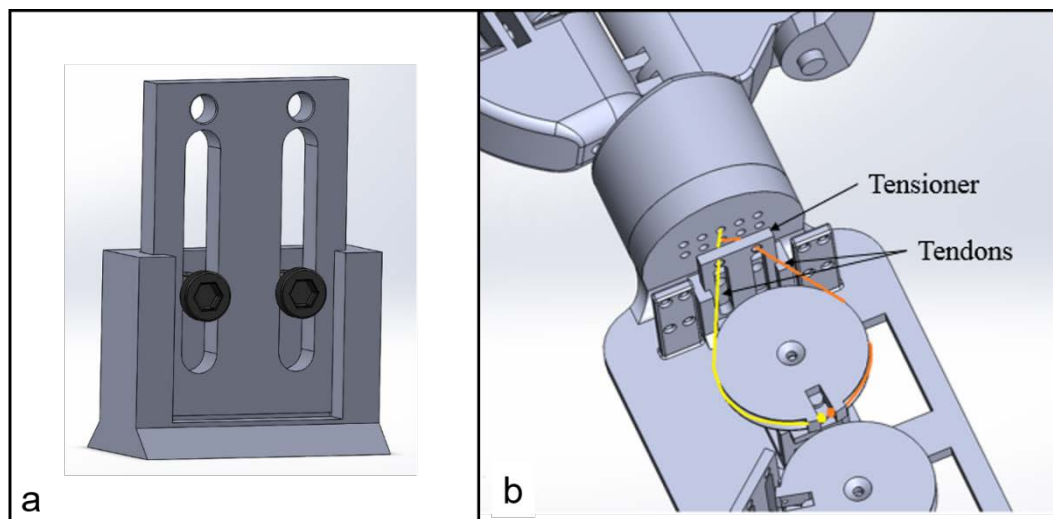

Fig. 4.6. (a) Tensioner, (b) Tendon routing

4.6 Actuation

Fingers of the hand are actuated using five servomotors placed in hand. The movement of each finger is achieved by pulling of the tendons passing through all fingers. Actuation method is explained in the sections below.

4.6.1. Tendon Drives

The tendons used in this design are braided fishing lines. These tendons tied to the custom 3D-printed servo pulleys as shown below. First, these tendons pass through one of the ten holes of wrist and then are passed through the tensioner attachment to the servo pulleys. The servo motor rotates in one direction to achieve flexion movement (closing of the finger), while it rotates in the opposite direction to achieve extension movement (opening of the finger). Figure 4.8 shows the artificial tendon drive for the middle finger. The thumb, index, middle, ring, and pinky fingers are driven by individual servo motors.

4.6.2 Servomotor Placement

The forearm of this design is simple, consisting of slots for five servomotors and few poles with holes for routing the tendons to each servomotor. All the servomotors are placed one behind the other. Separate attachments for the tendon routing (tensioner) are mounted later. This forearm design takes the place of radius and ulna bones of hand. Particulars of these bones are not considered as a part of design (See Figure 4.7).
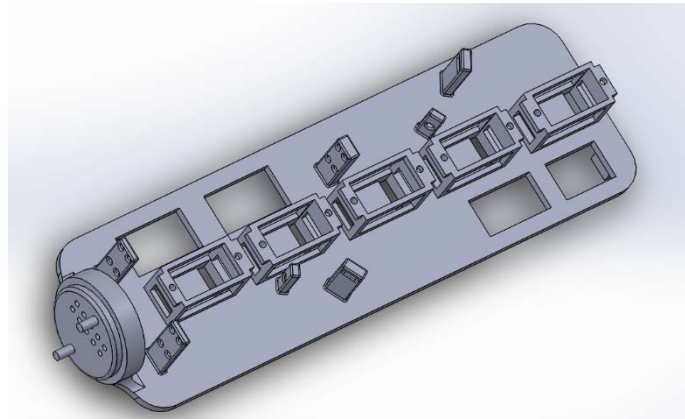
Fig. 4.7. The design for motor placement

4.7 Calculations of Force in a Finger

A finger moves in two directions, flexion and extension. Force calculations during both these movements are required. Let us consider the situation in which the index finger is fully extended and a force is applied near the tip of the finger.

$$\text{Moment} = (\text{Force}) \times (\text{Perpendicular Distance})$$
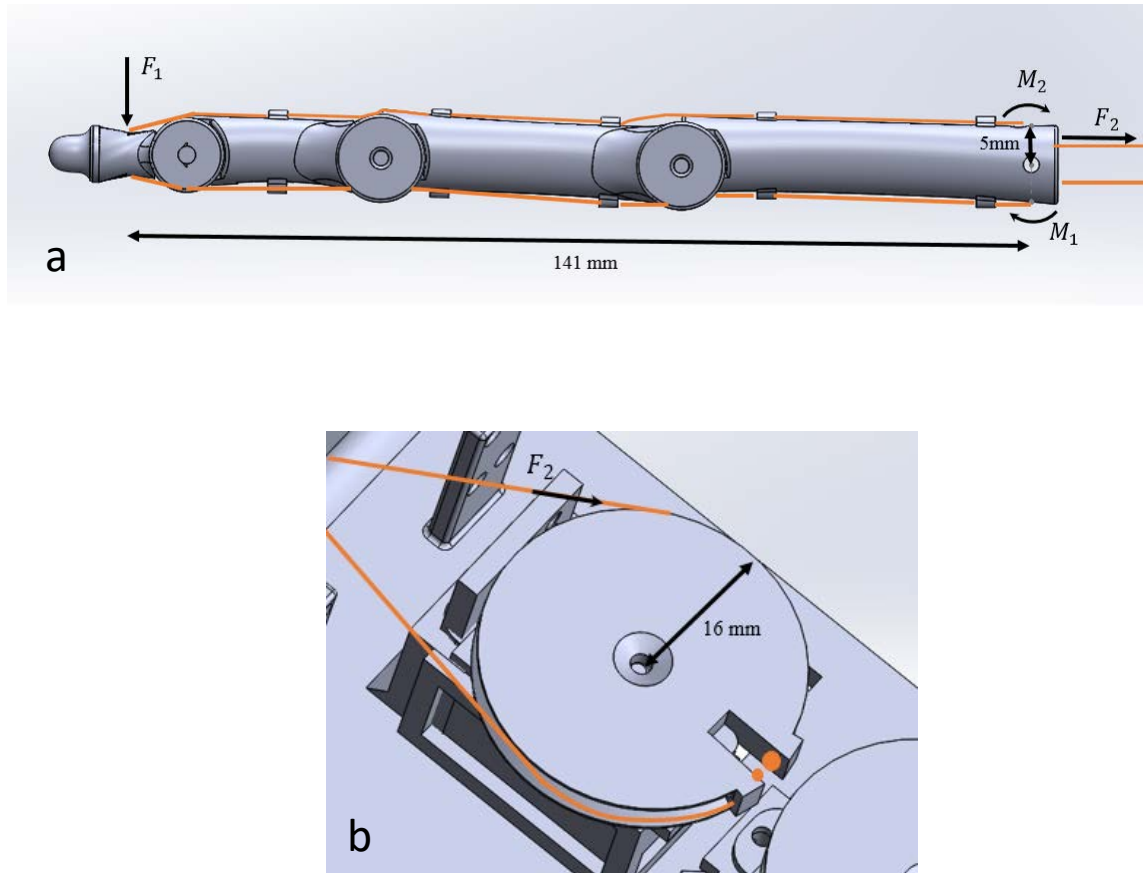
$$M = F \cdot d$$

(5.1)

Fig. 4.8. (a) Forces on Index Finger, (b) Force acting at the pulley

Moment is created by the tendons about each joint in the finger. The moment about the joint at the base of metacarpal bone will be the greatest since it is the furthest away from the applied force. Therefore, it is the turning force at this joint that limits the load one can lift at the tip of the finger. The moments M1 and M2 will balance out at the point where the maximum load can be lifted. The tensile force in the tendon can be calculated as below. The stall torque (maximum turning force) of the servomotor S3114, used in this design, is 1.5 kg-cm (0.147 Nm).

$$F_2 = 0.147 \text{ Nm} / 0.016 \text{ m} = 9.2 \text{ N} \qquad (5.2)$$

where F_2 represents the tension in the tendon.

$$F_1 D_1 = F_2 D_2$$

$$F_1 = \frac{(9.2 \text{ } N)5mm}{141mm} = 0.326 \text{ N} \qquad (5.3)$$

A force of 0.326 N can be applied at each fingertip when fully extended or 33 gms mass can be lifted during extension position. As the finger starts the flexion movement the perpendicular distance between the metacarpal joint and the applied load decreases resulting in a reduced moment about that joint. This means the finger tips apply more force as they continue flexion movement. In a complete flexed finger position, the applied force to the index finger would be acting in similar fashion to Figure 4.9.
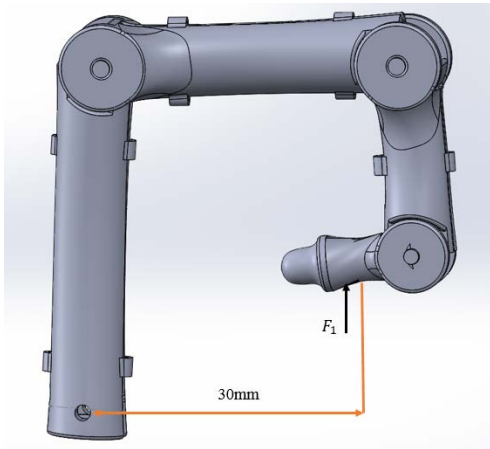

Fig. 4.9. Forces on the index finger while in flexion during grasp

In this position, the perpendicular distance from the applied force to the joint is smaller than that of extended position. Therefore, the fingertip can apply a larger force.

4.8 3D Printing and Assembly

The assembly CAD model of the synthetic hand is shown in Figure 4.10. The figure shows a close resemblance of the synthetic hand design to a human hand. The hand assembly consisted of a total of 38 parts and 20 pins. All these parts are 3D printed and assembled.
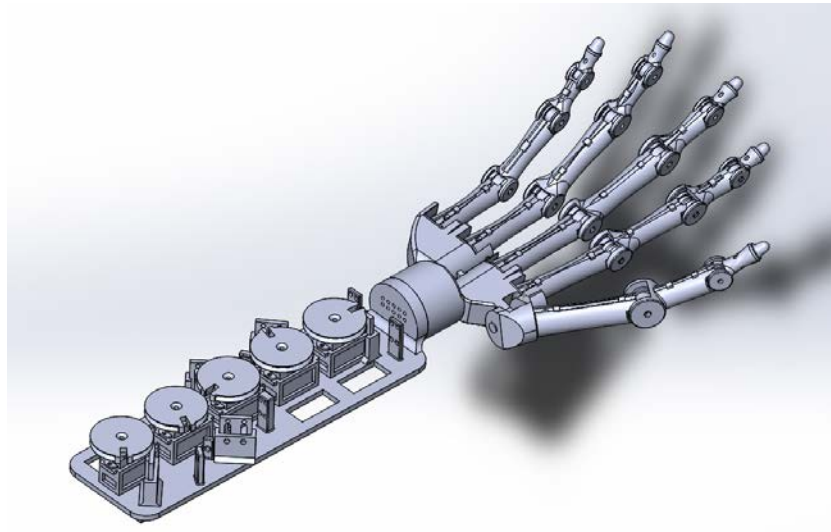

Fig. 4.10. CAD model of anthropomorphic robotic hand designed in Solidworks

TABLE 5

DIMENSIONS OF THE DESIGNED HAND

Finger	Total Length(mm)	Distal Phalange (mm)	Middle Phalange (mm)	Proximal Phalange (mm)	Metacarpal (mm)
Index	189	22	31	58	78
Middle	206.48	23	39.75	64.93	78.8
Ring	177.26	22.40	29.25	55.58	70.03
Pinky	159.54	22.44	24.63	44.47	68
Thumb	132.54	28.76	-	39.56	64.22

All the design parts including the pins were printed with the help of a 3D printer called a Objet30 Prime (Figure 4.11). The high quality mode of the printer was used to print all the parts so as to maximize the quality of the hand parts. The accuracy of the printer is 0.1mm. Figure 4.12 shows the 3D-printed parts of the index finger. These parts are ready for use after the removal of the support material by using a water jet machine.

3D printing or rapid prototyping is a technology for manufacturing in which the part is built by creating several layers of the printing material in succession. These layers are cured by UV lights. Material and the layer orientation of the design decides the strength of the 3D printed part. Figure 4.13 shows the assembly of the anthropomorphic hand.

Fig. 4.11. 3D Printer Objet 30 Prime

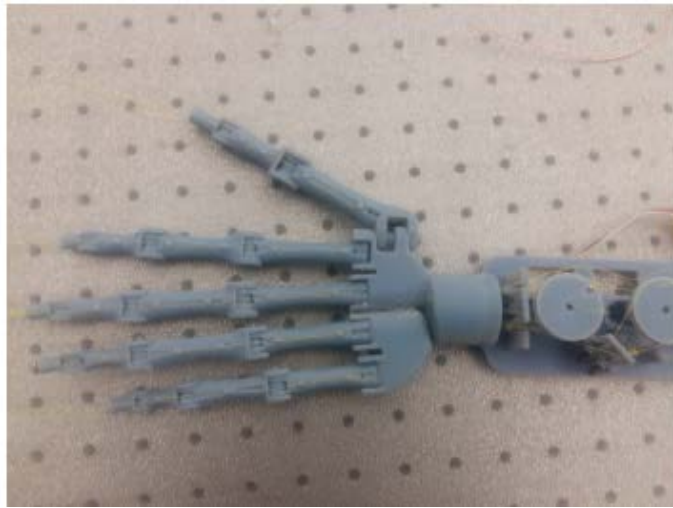Fig. 4.12. (a) 3D Printed index finger, (b) Fingers covered in support material

Fig. 4.13. Assembly of the robotic hand

CHAPTER 5

EXPERIMENTAL VALIDATION

Initially, the working of a prototype of one finger was tested to investigate whether the desired functionality can be achieved by using the proposed design of various finger segments, tendon-routing, and servomotor placement. This enables perfecting the design by making necessary modifications until a well-working prototype is achieved. This saves the time and effort that may be spent in proceeding along a wrong path, which will eventually end up in the failure of the overall design. The goal of this test was to check the finger for its intended movement at every joint of the finger.

5.1 Experimental Setup

A small testing assembly, consisting of servomotor, pulley for tendon routing, and tensioner to adjust the tension in the tendons, was designed and built (Figure 5.1). In this case, an index finger was tested successfully with the help of servomotor and Arduino-based control. But there was some problem with the tensioning of the tendon, it had less tension. To solve this problem, a spring attachment was designed so that it will allow for an adjustment of the tension of the tendon. Even this spring attachment did not serve the purpose of tensioning. To fix the problem, a spring attachment was replaced with a tensioner to have the tendons routed in appropriate way, while maintaining tendons on the pulley with required tension in tendons was successfully achieved by attaching a spring in series with the tendons (Figure 5.2).
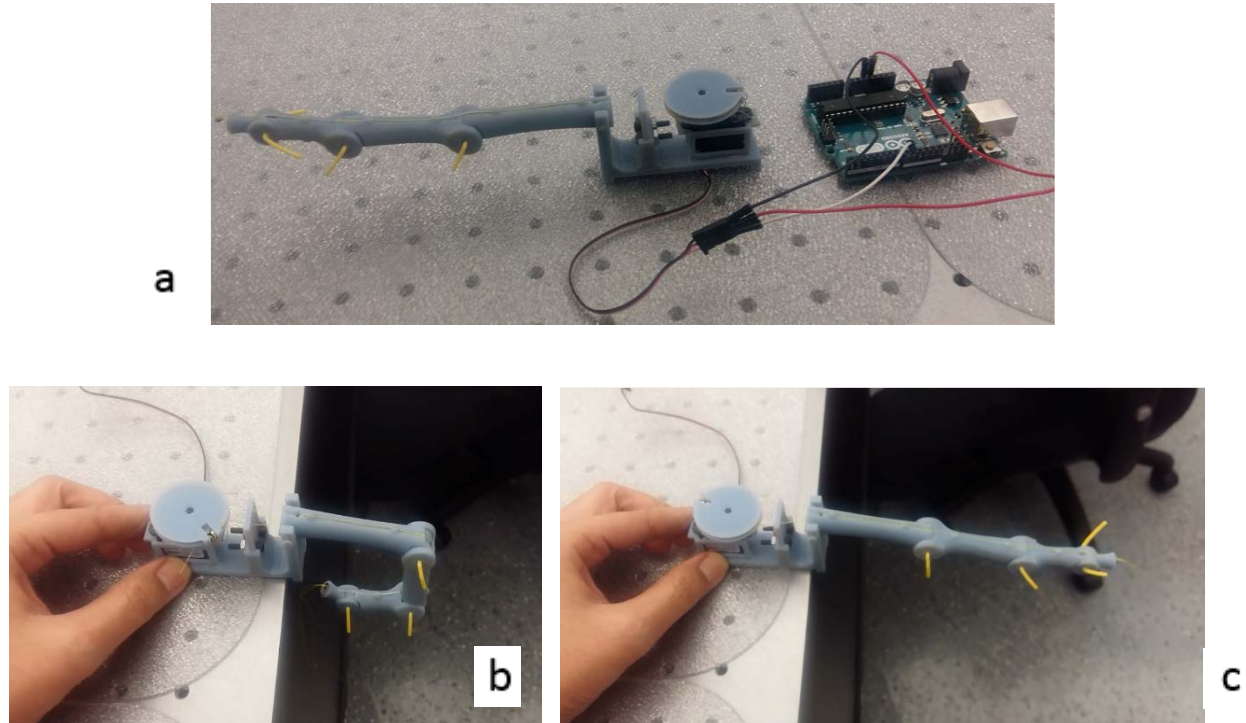
Fig. 5.1. (a) The test assembly for testing the index finger of the design,(b) Flexion

movement (c) Extension movement
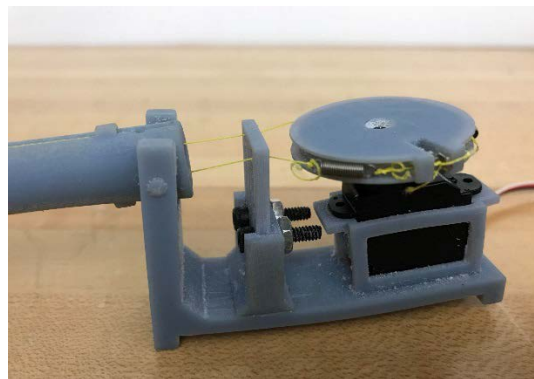
Fig. 5.2. Use of spring in tendon routing

After successfully testing an index finger, all other fingers are 3D-printed and assembled

together with the wrist and forearm parts. Figure 5.3, below, shows the whole assembly of the

hand design and test setup. All ten tendons necessary for the motion of five finger are passed through the tendon route provided. The thumb, index, and middle, ring, and pinky fingers each move independently. The hand was tested for the required motion of all fingers.

Fig. 5.3. The test assembly for testing the whole hand design

Fig. 5.4. Comparison with a real hand

Fig. 5.5. Hand with flexion of each finger

5.1.1 Synthetic Hand Specifications

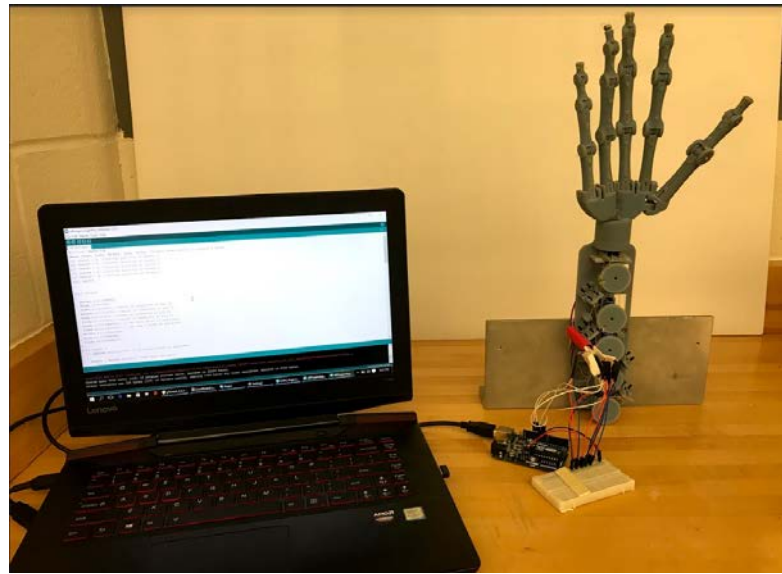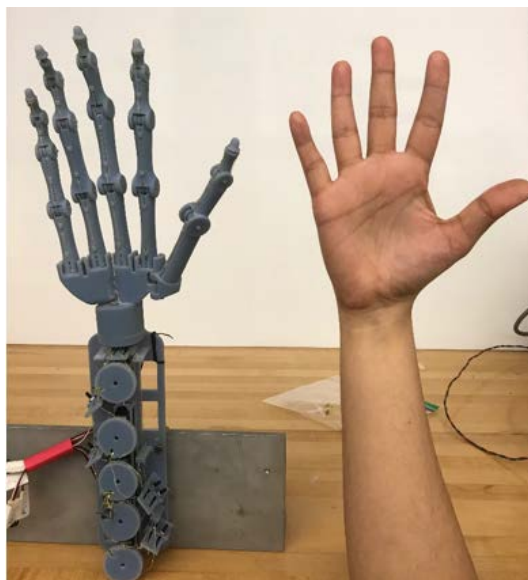The synthetic hand consists of five fingers including index, middle, ring, pinky, and thumb. Each finger moves independently with the help of separate tendons. These tendons are activated through five servomotors. The wrist is fixed as it does not have any DOF.

5.1.2 3D Printer Material

The 3D printer uses Polyjet technology, which 3D prints objects by jetting fine droplets of photopolymers that solidify once they are exposed to ultraviolet light. The properties of Polyjet material used for 3D printing are given in Table 6. The specific material used for this purpose is VeroBlue, which is a rigid plastic. This material is opaque blue and is good for fine feature detail [50]. A highlight of the material is a layer thickness of 0.0006 in., the thinnest available material for the printer, giving a better raw surface finish.

TABLE 6

Hand Specification

Properties	Description
Number of Fingers	5
Total Weight	286 gms
Material	Polyjet Material
Activation	Servomotors
Tendons	Braided fishing line

Rigid opaque photopolymers are generally stronger and stiffer when compared to a common engineering plastic like standard ABS thermoplastic in terms of tensile strength, flex strength, and flex modulus. The total profile of characteristics of rigid opaque materials is more comparable to an acrylic than to an ABS, PC, polypropylene, or polyamide.

TABLE 7

Physical Properties of VeroBlue Polyjet material

Physical Property	Metric	Unit
Tensile Strength	7250-8700	psi
Elongation at break	15-25	%
Modulus of elasticity	2000-3000	Psi
Hardness	83-86	(Shore D)
Heat deflection @ 264 psi	113-122	°F
Flexural modulus	1900-2500	MPa

5.1.3 Servomotor

The servomotors used for actuation are Servo s3114. The main reason behind the usage is that it can be easily accommodated in a very small space that is available in the hand.

TABLE 8

Specification of servomotor:

Dimension	.86" x 0.43"x .78" (21.8 x 11 x 19.8mm)
No-Load Speed (4.8V)	0.10sec/60°
No-Load Speed (6.0V)	0.09sec/60°
Stall Torque (4.8V)	20.8 oz/in. (1.5kg.cm)
Stall Torque (6.0V)	23.5 oz/in. (1.7kg.cm)
Gear Type	Straight Cut Spear

5.1.4 Finger Movements

It is also important to check how well the finger moves. The smoothness of the finger movement depends on several factors like servo control, friction between the moving parts, friction for the tendon routing, and the tension in the tendons. All the fingers of this design move relatively smoothly. The friction between the moving parts (bone segments) and also between bone segment and pin do not hinder the movement greatly. The middle finger moves smoothly along the whole range of motion they are designed for as it is attached the closest servo to the wrist. But as we move on to the next servo motors, the number of points of contact between the tendon and the routing channel and small directional changes increase, which results in increasing the tendon friction.

5.1.4 Pulley Dimensions

Dimensions of the pulley are also very crucial for the full finger movement. The initial design of the pulley had insufficient radius, causing the finger to achieve around half of the range of motion. Required radius for the servo pulley is calculated in following way. The middle finger of the design was chosen to calculate the pulley radius as it the longest finger of design having

highest movement. The total thread displacement during the flexion and extension movement of the middle finger is measured to be 84.9 mm. This distance is equal to the perimeter of pulley.

$$l = 2\pi r$$

$$r = \frac{84.9}{2\pi} = 13.51 \text{mm}$$
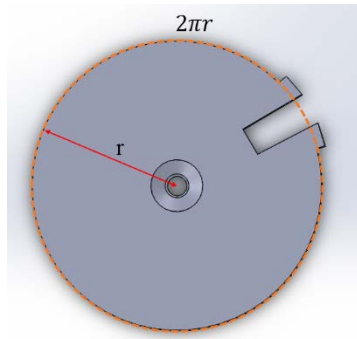
(5.1)

Fig. 5.6. Pulley dimension

5.2 Grasp Classification

A human hand can perform various types of grasps. A grasp taxonomy enables us to identify a peculiar grasp and its generic grasp type. Task requirements and geometry are very essential for any kind of grasp. Usually the specific nature of grasp depends on the basic geometry of the object being grasped. Even with the same geometry, different grasps may be required depending on the task to perform. Figure 5.7 depicts all possible sixteen hand postures for grasp that a human hand can perform [51]. Cutkosky divided the grasps such that it represents power and precision grasps from left to right while from top to bottom represents the geometry. The grasps are classified into six types: cylindrical, tip, hook, palmar, spherical, and lateral. The

proposed anthropomorphic robotic hand was tested to perform some of the basic grasps given in
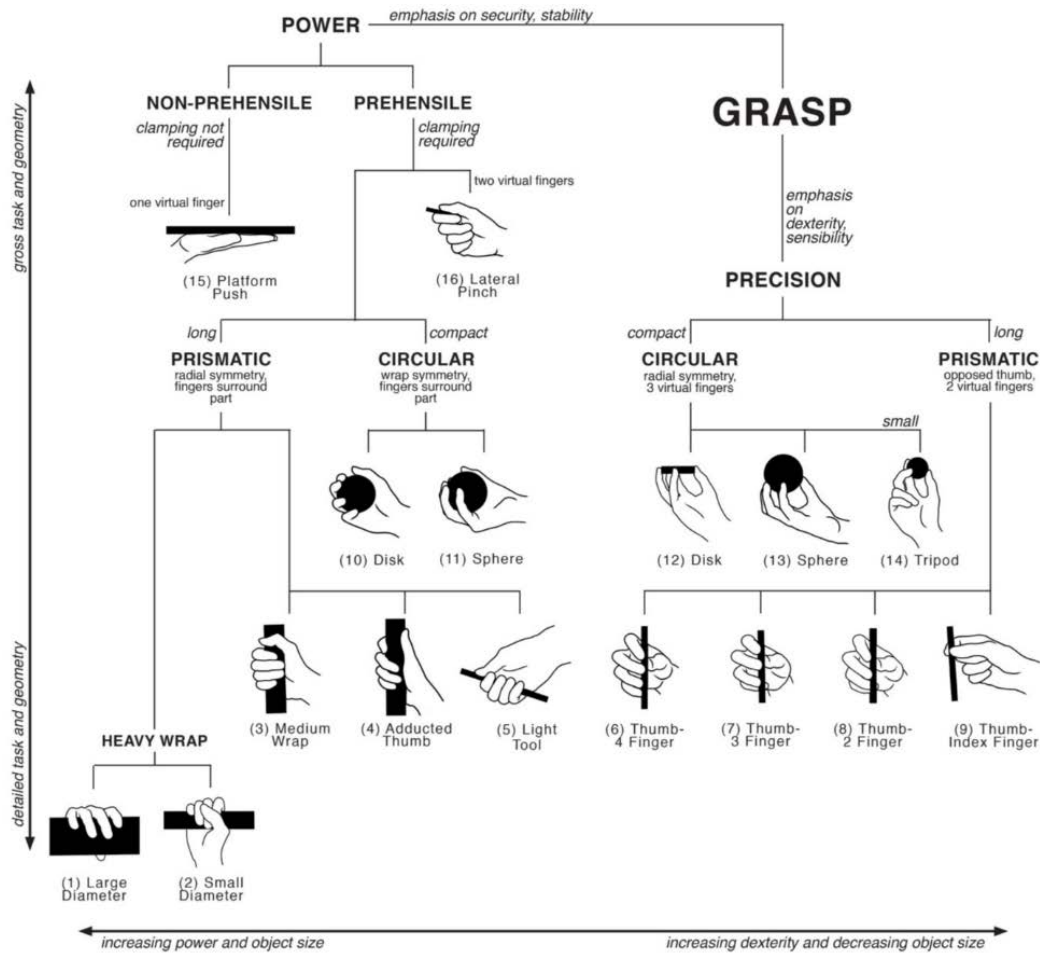
Figure 5.7.

Fig. 5.7. The human hand grasps [18, 51]

5.3 Grasping Experiments

The overall performance of the robotic hand was evaluated by testing some of the grasps defined earlier. Each grasp experiment was conducted by holding an object in front of the hand, near the palm region, and actuating all the fingers to perform flexion, and thereby, achieve a grasping (closing) behavior. The robotic hand successfully demonstrated rectangular, disc, cylindrical, and spherical grasp patterns as shown in Figure 5.8. Snapshots from a video footage of the hand grasping a wooden block, insulation tape roll, a cardboard tube, and a spherical ball are shown in Figure 5.9.

Rectangle

Disc

Cylinder

Sphere

Fig. 5.8. Different grasps performed with hand according to the shapes of objects
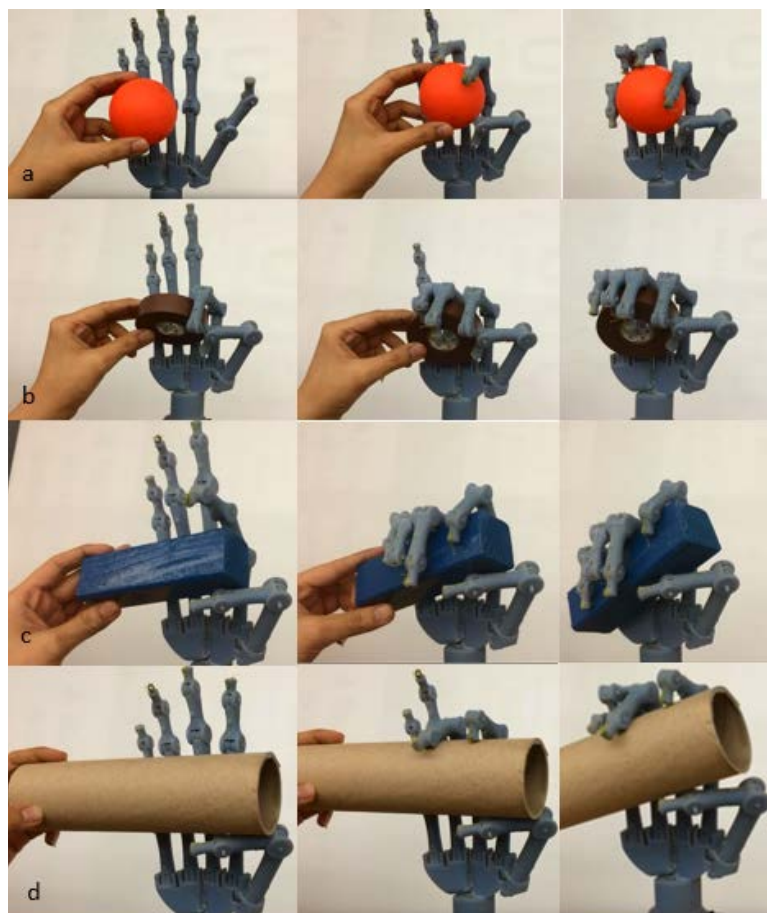
grasped

Fig. 5.9. Stages of grasping the objects a: Sphere b: Disc Rectangular block d: Cylinder

CHAPTER 6

CONCLUSIONS AND FUTURE WORK

This thesis involved the design of a robotic hand by borrowing inspiration from the anthropomorphic structure of a human hand. The goal was to develop a systematic methodology that enables us to custom-build the prosthesis to match the specific requirements of a person with upper extremities. A low-cost and light-weight anthropomorphic hand was designed and 3D-printed by making appropriate approximations and simplifications. This design represents the skeleton structure of a hand.

Though the robotic hand met with success in showcasing few grasping postures, there is still scope for improvements in the near future. Some important directions for future work include:

1) Introducing rotational DOFs in the wrist in order to enhance the hand dexterity and endow an ability to reduce the shocks generated from impacts

2) Embedding sensors like tactile, pressure, and slip sensors

3) Use of natural looking skin on the top of hand

4) Design of an arm attachment to fit the robotic prosthetic hand to the amputated limb of the patient, and

5) Changes in the wrist design to overcome friction issues in tendon-routing.

With future improvements to the current design, this research is expected to contribute significantly to field of prostheses by enabling rapid design and fabrication of robotic prostheses to match the custom requirements of hand-amputees.

REFERENCES

[1]   C. Medynski and B. Rattray, "Bebionic Prosthetic Design," in *MyoElectric Controls/Powered Prosthetics Symposium Fredericton*, New Brunswick, Canada, 2011.

[2]   (2009, 2 March). *Touch Bionics Inc*. Available: https://www.touchbionics.com/

[3]   S. A. Dalley, T. E. Wiste, T. J. Withrow, and M. Goldfarb, "Design of a Multifunctional Anthropomorphic Prosthetic Hand with Extrinsic Actuation," *IEEE/ASME Transactions on Mechatronics,* vol. 14, no. 6, pp. 699-706, 2009.

[4]   (2008). *Shadow Robot Company*. Available: https://www.shadowrobot.com/

[5]   S. C. Jacobsen, E. K. Iversen, D. F. Knutti, R. T. Johnson, and K. B. Biggers, "Design of the Utah/M.I.T. Dextrous Hand," *IEEE,* vol. 3, pp. 1520-1532, 1986.

[6]   M. A. Diftler and R. O. Ambrose, "Robonaut: A Robotic Astronaut Assistant," in *6th International Symposium on Artificial Intelligence and Robotics & Automation in Space: i-SAIRA*, Canadian Space Agency,St-Hubert, Quebec, Canada, 2001.

[7]   J. Ueda, M. Kondo, and T. Ogasawara, "The Multifingered NAIST Hand System for Robot In-hand Manipulation," *Mechanism and Machine Theory,* vol. 45, no. 2, pp. 224-238, 2010/02/01/ 2010.

[8]   F. Lotti, P. Tiezzi, G. Vassura, L. Biagiotti, G. Palli, and C. Melchiorri, ""Development of UB Hand 3: Early Results"," in *Proceedings of the 2005 IEEE International Conference on Robotics and Automation*, 2005, pp. 4488-4493.

[9]   (2012). *Ottobok*. Available: https://www.ottobock.com/en/

[10]   D. H. Lee, J. H. Park, S. W. Park, M. H. Baeg, and J. H. Bae, "KITECH-Hand: A Highly Dexterous and Modularized Robotic Hand," *IEEE/ASME Transactions on Mechatronics,* vol. 22, no. 2, pp. 876-887, 2017.

[11]   T. Mouri, H. Kawasaki, K. Yoshikawa, J. Takai, and S. Ito, "Anthropomorphic Robot Hand: Gifu Hand III," *Proc. Int. Conf. Control, Autom. Syst.,* pp. 1288-1293, 2001.

[12]   Z. Xu and E. Todorov, "Design of a Highly Biomimetic Anthropomorphic Robotic Hand towards Artificial Limb Regeneration," presented at the IEEE International Conference on Robotics and Automation (ICRA), Stockholm, 2016.

[13]   C. L. Taylor and R. J. Schwarz, "The Anatomy and Mechanics of the Human Hand," Artif Limbs., 1955, pp. 22–35. [Online]. Available.

[14]   F. Cordella *et al.*, "Literature Review on Needs of Upper Limb Prosthesis Users," (in English), *Frontiers in Neuroscience,* Review vol. 10, no. 209, 2016-May-12 2016.

[15]   S. Schulz, C. Pylatiuk, and G. Bretthauer, "A New Ultralight Anthropomorphic Hand," in *Proceedings 2001 ICRA. IEEE International Conference on Robotics and Automation (Cat. No.01CH37164)*, 2001, vol. 3, pp. 2437-2441 vol.3.

[16]   (2013). *Vincent Hand*. Available: https://vincentsystems.de/en/

[17]   M. Controzzi, C. Cipriani, and M. C. Carrozza, "Design of Artificial Hands: A Review," in *The Human Hand as an Inspiration for Robot Hand Development*, R. Balasubramanian and V. J. Santos, Eds. Cham: Springer International Publishing, 2014, pp. 219-246.

[18]   V. J. S. Ravi Balasubramanian, *The Human Hand as an Inspiration for Robot Hand Developement*. New York: Springer, 2014.

[19]   B. T. Carlsen, P. Prigge, and J. Peterson, "Upper Extremity Limb Loss: Functional Restoration from Prosthesis and Targeted Reinnervation to Transplantation," *Journal of Hand Therapy,* vol. 27, no. 2, pp. 106-114.

[20]   E. Y. Chao, J. D. Opgrande, and F. E. Axmear, "Three-dimensional Force Analysis of Finger Joints in Selected Isometric Hand Functions," *Journal of Biomechanics,* vol. 9, no. 6, pp. 387-IN2, 1976/01/01/ 1976.

[21]   E. Biddiss, D. Beaton, and T. Chau, "Consumer Design Priorities for Upper Limb Prosthetics," *Disability and Rehabilitation: Assistive Technology,* vol. 2, no. 6, pp. 346-357, 2007/01/01 2007.

[22]   D. J. Atkins, D. C. Y. Heard, and W. H. Donovan, "Epidemiologic Overview of Individuals with Upper-Limb Loss and Their Reported Research Priorities," *JPO: Journal of Prosthetics and Orthotics,* vol. 8, no. 1, pp. 2-11, 1996.

[23]   F. Chen Chen, S. Appendino, A. Battezzato, A. Favetto, M. Mousavi, and F. Pescarmona, "Constraint Study for a Hand Exoskeleton: Human Hand Kinematics and Dynamics," *Journal of Robotics,* vol. 2013, p. 17, 2013, Art. no. 910961.

[24]   DEKA Research and Development Corp. (2008, 2 March). Available: http://www.dekaresearch.com/

[25]   T. Nicholas and S. Priya, "Design and Implementation of a Dextrous Anthropomorphic Robotic Typing (DART) Hand," *Smart Materials and Structures,* vol. 20, 2011.

[26] F. Simone, A. York, and S. Seelecke, "Design and Fabrication of a Three-finger Prosthetic Hand using SMA Muscle Wires," in *SPIE Smart Structures and Materials + Nondestructive Evaluation and Health Monitoring*, 2015, vol. 9429, p. 8: SPIE.

[27] F. Rothling, R. Haschke, J. J. Steil, and H. Ritter, "Platform Portable Anthropomorphic Grasping with the Bielefeld 20-DOF Shadow and 9-DOF TUM Hand," in *2007 IEEE/RSJ International Conference on Intelligent Robots and Systems*, 2007, pp. 2951-2956.

[28] J. T. Belter, J. L. Segil, A. M. Dollar and R. F. Weir, "Mechanical Design and Performance Specifications of Anthropomorphic Prosthetic Hands: A Review," *Journal of Rehabilitation Research and Development; Washington,* vol. 50, no. 5, pp. 599-618, 2013.

[29] T. Laliberte, L. Birglen, and C. Gosselin, *Underactuation in Robotic Grasping Hands* (no. 3). 2002, pp. 1-11.

[30] C. S. Lovchik and M. A. Diftler, "The Robonaut Hand: A Dexterous Robot Hand for Space," in *Proceedings 1999 IEEE International Conference on Robotics and Automation (Cat. No.99CH36288C)*, 1999, vol. 2, pp. 907-912 vol.2.

[31] I. Yamano and T. Maeno, "Five-fingered Robot Hand using Ultrasonic Motors and Elastic Elements," in *Proceedings of the 2005 IEEE International Conference on Robotics and Automation*, 2005, pp. 2673-2678.

[32] M. C. Carrozza, G. Cappiello, S. Micera, B. B. Edin, L. Beccai, and C. Cipriani, "Design of a Cybernetic Hand for Perception and Action," *Biological Cybernetics,* vol. 95, no. 6, p. 629, December 06 2006.

[33] V. Bundhoo and E. J. Park, "Design of an Artificial Muscle Actuated Finger towards Biomimetic Prosthetic Hands," in *ICAR '05. Proceedings, 12th International Conference on Advanced Robotics, 2005*, 2005, pp. 368-375.

[34] Z. Xu, V. Kumar, Y. Matsuoka, and E. Todorov, "Design of an Anthropomorphic Robotic Finger System with Biomimetic Artificial Joints," presented at the 4th IEEE RAS & EMBS International Conference on Biomedical Robotics and Biomechatronics (BioRob), Rome, 2012.

[35] G. A. Pratt and M. M. Williamson, "Series Elastic Actuators," in *Proceedings 1995 IEEE/RSJ International Conference on Intelligent Robots and Systems. Human Robot Interaction and Cooperative Robots*, 1995, vol. 1, pp. 399-406 vol.1.

[36]   R. V. Ham, T. G. Sugar, B. Vanderborght, K. W. Hollander, and D. Lefeber, "Compliant Actuator Designs," *IEEE Robotics & Automation Magazine,* vol. 16, no. 3, pp. 81-94, 2009.

[37]   G. ElKoura and K. Singh, "Handrix: Animating the Human Hand," presented at the Proceedings of the 2003 ACM SIGGRAPH/Eurographics symposium on Computer animation, San Diego, California, 2003.

[38]   J. N. Ingram, K. P. Körding, I. S. Howard, and D. M. Wolpert, "The Statistics of Natural Hand Movements," *Experimental Brain Research,* vol. 188, no. 2, pp. 223-236, June 01 2008.

[39]   V. K. Nanayakkara, G. Cotugno, N. Vitzilaios, D. Venetsanos, T. Nanayakkara, and M. N. Sahinkaya, "The Role of Morphology of the Thumb in Anthropomorphic Grasping: A Review," (in English), *Frontiers in Mechanical Engineering,* Review vol. 3, no. 5, 2017-June-30 2017.

[40]   T. D. White and P. A. Folkens, "Bone Biology and Variartion," in *The Human Bone Manual*, 2005.

[41]   S. J. L. Lynette A. Jones, *Human Hand Function*. New York: Oxford University Press, Inc, 2006.

[42]   J. C. Colditz. (2016, 03/02). *A White Paper: Describing the Stabilizing Mechanism of the Push MetaGrip*. Available: http://www.sportstek.net/pushcmcwhitepaper.htm

[43]   F. K. Morton DA, Albertine KH. (2011, February 28). *The Big Picture: Gross Anatomy*. Available: http://accessphysiotherapy.mhmedical.com/content.aspx?sectionid=40140043&bookid=381&jumpsectionID=40142128&Resultclick=2

[44]   B. Buchholz and T. J. Armstrong, "A Kinematic Model of the Human Hand to Evaluate its Prehensile Capabilities," *Journal of Biomechanics,* vol. 25, no. 2, pp. 149-162, 1992/02/01/ 1992.

[45]   K. N. An, E. Y. Chao, W. P. Cooney, and R. L. Linscheid, "Normative Model of Human Hand for Biomechanical Analysis," *Journal of Biomechanics,* vol. 12, no. 10, pp. 775-788.

[46]   (2015). *"Hand Tendon Repair"*. Available: https://www.nhs.uk/conditions/hand-tendon-repair/

[47]   M. Nordin and V. H. Frankel, *Basic Biomechanics of the Musculoskeletal System*, 3rd ed. Baltimore,Maryland: Lippincott Williams and Wilkins, 2001, p. 467.

[48]   J. J. Craig, *Introduction to Robotics: Mechanics and Control*. Pearson/Prentice Hall, 2005.

[49]   G. Langevin. Available: http://inmoov.fr/

[50]   (2018). *Polyjet Materials*. Available: https://www.stratasysdirect.com

[51]   M. R. Cutkosky, "On Grasp Choice, Grasp Models, and the Design of Hands for Manufacturing Tasks," *IEEE Transactions on Robotics and Automation,* vol. 5, no. 3, pp. 269-279, 1989.

VITA

Manali Bapurao Bhadugale

238 Kaufman Hall
Mechanical and Aerospace
Department
Old Dominion University
Norfolk, VA 23529

Education:

2018	**M.S.**	Mechanical & Aerospace Engineering	Old Dominion University
2011	**MBA**	Human Resource & Systems	Solapur University, India
2009	**B. E.**	Production Engineering	Solapur University, India